DNA Methylation Mark in Mitochondrial DNA

By

Fadumo Osman

A Thesis submitted to the Faculty of Graduate Studies of

The University of Manitoba

in partial fulfillment of the requirements of the degree of

MASTER OF SCIENCE

Department of Biochemistry and Medical Genetics

University of Manitoba

Winnipeg

This thesis should be cited as follows:

Osman, F., Dolinsky, V.W., Karakack, T., and Davie, J.R. (2020) DNA Methylation Mark in Mitochondrial DNA.

ABSTRACT

DNA methylation, 5-methylcytosine (5-mC), is a key epigenetic modification involved in gene regulation found in the nuclear genome of various organisms. Interestingly, mitochondrial DNA (mtDNA) has also been found to be modified by 5-mC. Research to determine the functional relevance and identify players regulating mtDNA methylation is receiving an ever-increasing interest.

This project is focused on understanding the mitochondrial methylation patterns in the normal physiological state using circulating $CD4^+$ and $CD8^+$ T cells as an informative study model. This knowledge might prove useful in understanding what arises during the pathological state. Moreover, mtDNA cellular content differs across tissue types depending on several factors including cellular energy demand which influence mtDNA replication and transcription rate. The objective of this study is to determine variations in mtDNA methylation of $CD4^+$ and $CD8^+$ T cells between healthy individuals as well as the ratio of mitochondrial/nuclear DNA in these cells to estimate whether the changes in methylation could possibly be contributed to changes in their relative mtDNA content.

In this study, blood samples from healthy donors were collected and $CD4^+$ and $CD8^+$ T cells were purified for analyses of 5-mC. The methylated DNA fragments enriched by methyl-CpG binding domain were sequenced and subsequent bioinformatic analysis involved preprocessing of the raw data, alignment of reads to the human mitochondrial genome and methylation peak calling. Methylation levels within the mitochondrial D-loop were then quantitatively evaluated by bisulfite-pyrosequencing. The results showed variations in the distribution of 5-mC in the different cell types and individuals, with the exception of 3' end in the terminal part of D-loop which appeared to be consistently methylated to a certain extent across

mtDNA with the average methylation level of ~ 1%. Additionally, quantitative PCR used to measure the ratio of mitochondrial/nuclear DNA showed no association between mtDNA methylation patterns and their relative mtDNA content. Overall, the low mtDNA methylation level detected deems it unlikely to have a major impact on mitochondrial function. Nevertheless, it is important to build on this knowledge, know the extent of mtDNA methylation in various cell types and design more comprehensive experiments to prove its biological significance.

ACKNOWLEDGEMENT

I wish to first express my deepest gratitude to my supervisor Dr. James Davie for the opportunity that was given to me. It has been an exciting learning journey and without his guidance, support and patience throughout my degree, this would not have been possible. His enthusiasm for science and love for sharing knowledge have always been a great source of motivation.

I whole-heartedly appreciate my advisory committee members, Dr. Vernon Dolinsky and Dr. Etienne Leygue for their valuable time, continuous support and encouragement. I also wish to extend my appreciation to Dr. Francis Amara and Dr. Jeffrey Wigle who have been there whenever I needed them providing me with great advice and guidance.

I would like to thank all members of the Davie lab in the past and present for their support during my training. I recognize the invaluable assistance I received from Ifeoluwa Adewumi, Dr. Ravinder Kaur, and Dr. Camila Lopez both inside and outside the lab. Special thanks to Ifeoluwa Adewumi for taking the time to teach me lab techniques when I first joined the lab. I greatly appreciate her informative input and willingness to always help me especially during stressful times.

I wish to pay my special regards to Dr. Ruey-Chyi Su and Dr. Meaghan Jones and their lab members whose help and training have been incredibly essential to the completion of my thesis. I would also like to thank Berardino Petrelli for being a great peer mentor during my years in the Department of Biochemistry and Medical Genetics. His personal and academic support made my graduate school experience smoother.

I wish to acknowledge the great love and endless support of my family, my beloved mother Halimo Sid, my cousin Hafsa Osman, and my partner Leo McKay. Their constant encouragement and belief in me kept me going through the ups and downs of this journey.

Finally, I extend my sincere gratitude to the University of Manitoba, Research Manitoba, Children's Hospital Research Institute of Manitoba and CancerCare. Without their support and funding, the goal of this project would not have been realized. Thank you!

TABLE OF CONTENTS

LIST OF TABLES

LIST OF FIGURES

LIST OF ABBREVIATIONS

5-caC	5-carboxylcytosine
5-fC	5-formylcytosine
5-gmC	β-glucosyl-5-methylcytosine
5-hmC	5-hydroxymethylcytosine
5-mC	5-methylcytosine
6-mA	N^6-methyladenosine
AIF	Apoptosis-inducing factor
APOBEC3	Apolipoprotein B mRNA editing enzyme catalytic polypeptide-like 3
ATCC	American Type Culture Collection
ATP	Adenosine triphosphate
BSA	Bovine serum albumin
$CD4^+$	Cluster of differentiation 4
$CD8^+$	Cluster of differentiation 8
CpA	Cytosine-phosphate-adenine
CpC	Cytosine-phosphate-cytosine
CpG	Cytosine-phosphate-guanine
CpT	Cytosine-phosphate-thymine
CSB	Conserved sequence block
D-loop	Displacement loop
DMEM	Dulbecco's modified Eagle’s medium
DMSO	Dimethyl sulfoxide
DNase	Deoxyribonuclease

DNMT	DNA methyltransferase
Drp1	Dynamin-related protein 1
ECL	Enhanced chemiluminescence
EDTA	Ethylenediaminetetraacetic acid
ENCODE	Encyclopedia of DNA elements
FBS	Fetal bovine serum
Fis1	Mitochondrial fission 1 protein
GAPDH	Glyceraldehyde 3-phosphate dehydrogenase
gDNA	Genomic deoxyribonucleic acid
GTPase	Guanosine triphosphate hydrolase
HDAC 2	Histone deacetylase 2
HSP	Heavy strand promoter
H-strand	Heavy strand
IGV	Integrative genomics viewer
LSP	Light strand promoter
L-strand	Light strand
M.CviPI	Chlorella virus GpC methyltransferase
M.SssI	Spiroplasma sp. strain CpG methyltransferase
MBD	Methyl CpG-binding domain
MBD-seq	Methyl-CpG binding domain sequencing
MeDIP-seq	Methylated DNA immunoprecipitation sequencing
MEK 1/2	MAPK or Erk kinases 1/2
Mfn	Mitofusin

MNase	Micrococcal nuclease
MTATP6	Mitochondrially encoded ATP Synthase subunit 6
MTATP8	Mitochondrially encoded ATP Synthase subunit 8
MTCO1	Mitochondrially encoded Cytochrome C Oxidase 1
MTCO2	Mitochondrially encoded Cytochrome C Oxidase 2
MTCYB	Mitochondrially encoded Cytochrome B
mtDNA	Mitochondrial deoxyribonucleic acid
mtDNMT1	Mitochondrially targeted isoform of DNA methyltransferase 1
mtIF	Mitochondrial translation initiation factor
MTND1	Mitochondrially encoded NADH dehydrogenase subunit 1
MTND4	Mitochondrially encoded NADH dehydrogenase subunit 4
MTND5	Mitochondrially encoded NADH dehydrogenase subunit 5
MTND6	Mitochondrially encoded NADH dehydrogenase subunit 6
MTRNR1	Mitochondrially encoded 12S rRNA
MTRNR2	Mitochondrially encoded 16S rRNA
mtSSB	Mitochondrial single-stranded DNA-binding protein
MTTA	Mitochondrially encoded tRNA alanine
MTTC	Mitochondrially encoded tRNA cysteine
MTTD	Mitochondrially encoded tRNA aspartic acid
MTTF	Mitochondrially encoded tRNA phenylalanine
MTTH	Mitochondrially encoded tRNA histidine
MTTK	Mitochondrially encoded tRNA lysine
MTTL2	Mitochondrially encoded tRNA leucine 2

MTTN	Mitochondrially encoded tRNA asparagine
MTTS1	Mitochondrially encoded tRNA serine 1
MTTS2	Mitochondrially encoded tRNA serine 2
MTTW	Mitochondrially encoded tRNA tryptophan
MTTY	Mitochondrially encoded tRNA tyrosine
NADH	Nicotinamide adenine dinucleotide
nDNA	Nuclear deoxyribonucleic acid
NP-40	Nonyl phenoxypolyethoxylethanol
NTC	Non-template control
NUMTs	Nuclear DNA sequences of mitochondrial origin
O_H	Heavy strand origin of replication
O_L	Light strand origin of replication
Opa1	Optic atrophy1 protein
oxBS-seq	Oxidative bisulfite sequencing
PAGE	Polyacrylamide gel electrophoresis
PBMCs	Peripheral blood mononuclear cells
PBS	Phosphate buffered saline
PE	Paired end
PIPES	Piperazine-1,4-bis (2-ethanesulfonic acid)
$PM_{2.5}$	Particulate matter < 2.5 µm in diameter
POLRMT	Mitochondrial RNA polymerase
POLγ	DNA polymerase gamma
RNase	Ribonuclease

SAM	S-adenosylmethionine
SDS	Sodium dodecyl sulfate
TAB-seq	Ten-eleven translocation dioxygenase-assisted bisulfite sequencing
TAS	Termination-associated sequences
TBE	Tris Borate EDTA
TBST	Tris-buffered saline tween-20
TE	Tris EDTA
TET	Ten-eleven translocation dioxygenase
TFAM	Mitochondrial transcription factor A
TFB2M	Mitochondrial transcription factor B2
$tRNA^{Phe}$	Transfer ribonucleic acid for phenylalanine
$tRNA^{Val}$	Transfer ribonucleic acid for valine
TSS	Transcription start site
ΔCt	Delta threshold cycle

CHAPTER ONE

1.0 INTRODUCTION

1.1. Mitochondria and Mitochondrial DNA

1.1.1. Mitochondrial Structure and Cellular Function

Mitochondria are complex intracellular membrane-bound organelles found in eukaryotic organisms and hypothesized to originate from α-proteobacteria through endosymbiosis in which the eukaryotic cell is formed from an archaebacterium engulfing an α-proteobacterium (Martin, Garg, & Zimorski, 2015). Mitochondria do not float freely in the cytosol and their position and movement are determined by the cytoskeleton mainly the intermediate filaments (Rappaport, Oliviero, & Samuel, 1998). Moreover, the number of mitochondria in a cell varies between different cell and tissue types depending on their energy demand to enable the fulfillment of specialized functions at regions of high-energy demand. Structurally, a mitochondrion is arranged into four distinct compartments. There is a matrix space containing mitochondrial ribosomes, and hundreds of enzymes of the citric acid cycle, also known as the tricarboxylic acid, and enclosed by an inner membrane containing the electron transport chain complexes and specific transporters for metabolites. Mitochondria also have a relatively permeable outer membrane and an intermembrane space.

Mitochondria are described to be the powerhouse of the cell due to their most prominent function of producing cellular chemical energy in the form of adenosine triphosphate (ATP) through aerobic respiration. Acetyl-coenzyme A in the mitochondrial matrix resulting from either pyruvate oxidation or fatty acid beta oxidation enters the citric acid cycle which generates the reduced cofactors nicotinamide adenine dinucleotide (NADH) and flavin adenine dinucleotide necessary for the oxidative phosphorylation via the electron transport chain (Wallace, Fan, &

Procaccio, 2010). The electron transport chain consists of multi-subunit protein complexes in the mitochondrial inner membrane including NADH dehydrogenase (complex I), succinate dehydrogenase (complex II), cytochrome c reductase/cytochrome b (complex III), cytochrome c oxidase (complex IV) and ATP synthase (complex V). An electrochemical proton gradient is generated across the inner membrane through the pumping of protons from the matrix into the intermembrane space. Eventually, the synthesis of ATP is powered by the proton potential difference (Wallace et al., 2010). Additionally, mitochondria serve as cellular calcium buffers by transporting calcium through mitochondrial Ca^{2+} uniporter on the inner membrane in case of a rise in its cytosolic concentration and temporarily storing it to maintain the calcium homeostasis (Baughman et al., 2011). In high energy-demand states, mitochondria communicate with the cytosol through calcium signaling as the resulting increase in the matrix calcium concentrations triggers the activation of the tricarboxylic acid cycle enzymes, eventually leading to an increase in ATP synthesis rate (Jacobson & Duchen, 2004). Moreover, mitochondria play a significant role in apoptosis through the changes in mitochondrial outer membrane permeability and release of apoptotic factors such as cytochrome c into the cytosol which in turn activate caspases (P. Li et al., 1997).

1.1.2. Mitochondrial Network Dynamics

Mitochondria do not exist as separate independent organelles, but rather as a highly connected and dynamic tubular network controlled by mitodynamins family of proteins through fusion and fission. Mitochondrial dynamics is critically important in many functions including the maintenance and quality control of mitochondria, mitochondrial genome stability, respiratory capacity and programmed cell death (Chan, 2012). Fusion involves the formation of a single mitochondrion from previously discrete and independent structures while fission results in the

separation of a single mitochondrion into two or more daughter organelles. While Mitofusins (Mfn1 and Mfn2), which are transmembrane GTPases, mediate mitochondrial outer membrane fusion in mammals (Santel & Fuller, 2001), optic atrophy 1 protein (Opa1) mediates mitochondrial inner membrane fusion (Delettre et al., 2000) (**Figure 1A**). Mitochondrial outer membrane fusion is almost always coordinated with inner membrane fusion, followed by the mixing of their intermembrane space and matrix contents (Karbowski et al., 2004). During fission (**Figure 1B**), dynamin-related protein (Drp1) is recruited from the cytosol to mediate mitochondrial division process through its candidate receptor Fis1 on the mitochondrial outer membrane leading to the constriction and scissoring of the mitochondrial tubule (Yoon, Krueger, Oswald, & McNiven, 2003). This protein is regulated by a range of protein modifications, including phosphorylation, ubiquitination, and sumoylation (C. R. Chang & Blackstone, 2010). It is important to mention that the balance between fusion and fission plays a key role in determining mitochondrial morphology and the resulting content exchange event helps maintaining a homogeneous mitochondrial population. Moreover, disruption of mitochondrial dynamics gives rise to several diseases. For example, Charcot-Marie-Tooth type 2A which is a peripheral neuropathy, and dominant optic atrophy are caused by heterozygous mutations in *MFN2* (Züchner et al., 2004) and *OPA1* (Delettre et al., 2000), respectively.

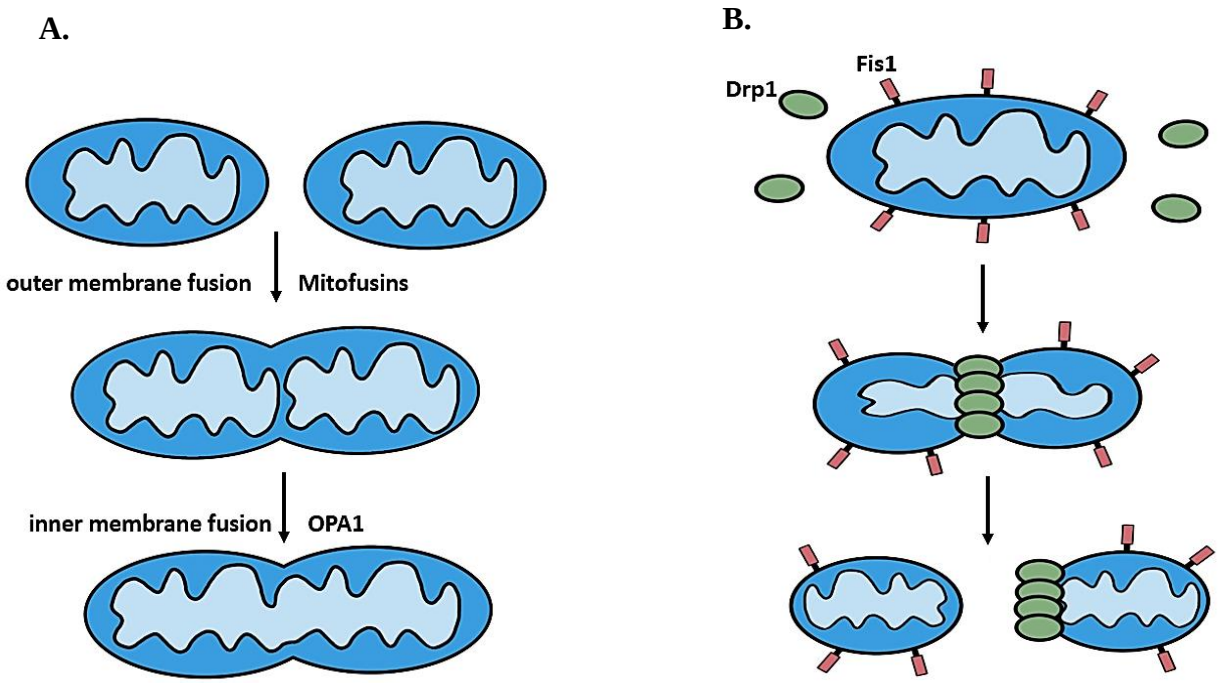

Figure 1. Mitochondrial dynamics.

A. Mitochondrial fusion machinery includes Mitofusins for outer membrane fusion and Opa1 for inner membrane fusion. **B.** During mitochondrial fission, Drp1 (*green ovals*) is recruited from the cytosol by Fis1 (*red projections*) on the mitochondrial outer membrane. Mitochondria undergo initial constriction (*not shown*) and Drp1 localization further constricts the mitochondrial tubules leading to their division. Drp1 molecules remain attached to one of the daughter mitochondria and are eventually disassembled.

1.1.3. Unique Features of Mitochondrial DNA

Mitochondria possess their own genome, referred to as mitochondrial DNA (mtDNA) (**Figure 2**). It has a circular, double-stranded structure consisting of heavy (H) strand and light (L) strand which can be separated by density centrifugation in alkaline cesium chloride gradients based on their base composition, with one strand being rich in guanines (Berk & Clayton, 1974). Mitochondrial DNA differs from nuclear DNA (nDNA) in following a non-Mendelian, inheritance pattern transmitted exclusively through maternal line (Giles, Blanc, Cann, & Wallace aD., 1980), lacking introns and possessing a polyploid nature with range of 2-10 copies per mitochondrion and 1000-10,000 copies per cell (Robin & Wong, 1988). However, not all mtDNA copies are identical or homoplasmic as mtDNA constantly acquire random mutations at a low level. The heteroplasmic state is when cells possess a mixture of two or more mitochondrial genotypes and it only leads to disease if mutations were above a minimal threshold level (Hayashi et al., 1991). The size of mtDNA in humans is 16,569 base pairs, encoding 37 genes, 22 of which are transfer RNAs (tRNAs), 2 ribosomal RNAs (rRNAs) and 13 messenger RNAs (mRNAs) of the oxidative phosphorylation subunits (S. Anderson et al., 1981). Additionally, it contains a ~1 kb noncoding regulatory region known as the displacement loop (D-loop) which harbors the H-strand promoter (HSP) and L-strand promoter (LSP) as well as H-strand origin of replication (O_H). The termination of H-strand replication from O_H at the termination-associated sequences (TAS) generates a short DNA fragment (~ 650 bp), known as 7S DNA which binds to the L-strand in place of the original H-strand (Doda, Wright, & Clayton, 1981). Consequently, the triple-stranded displacement loop structure is formed (Figure 2, top panel). However, the function and regulation of this event remain unknown. It was suggested that mtDNA helicase TWINKLE might be involved in regulating the 7S DNA levels in response to the cellular demand for mtDNA replication (Jemt et al., 2015).

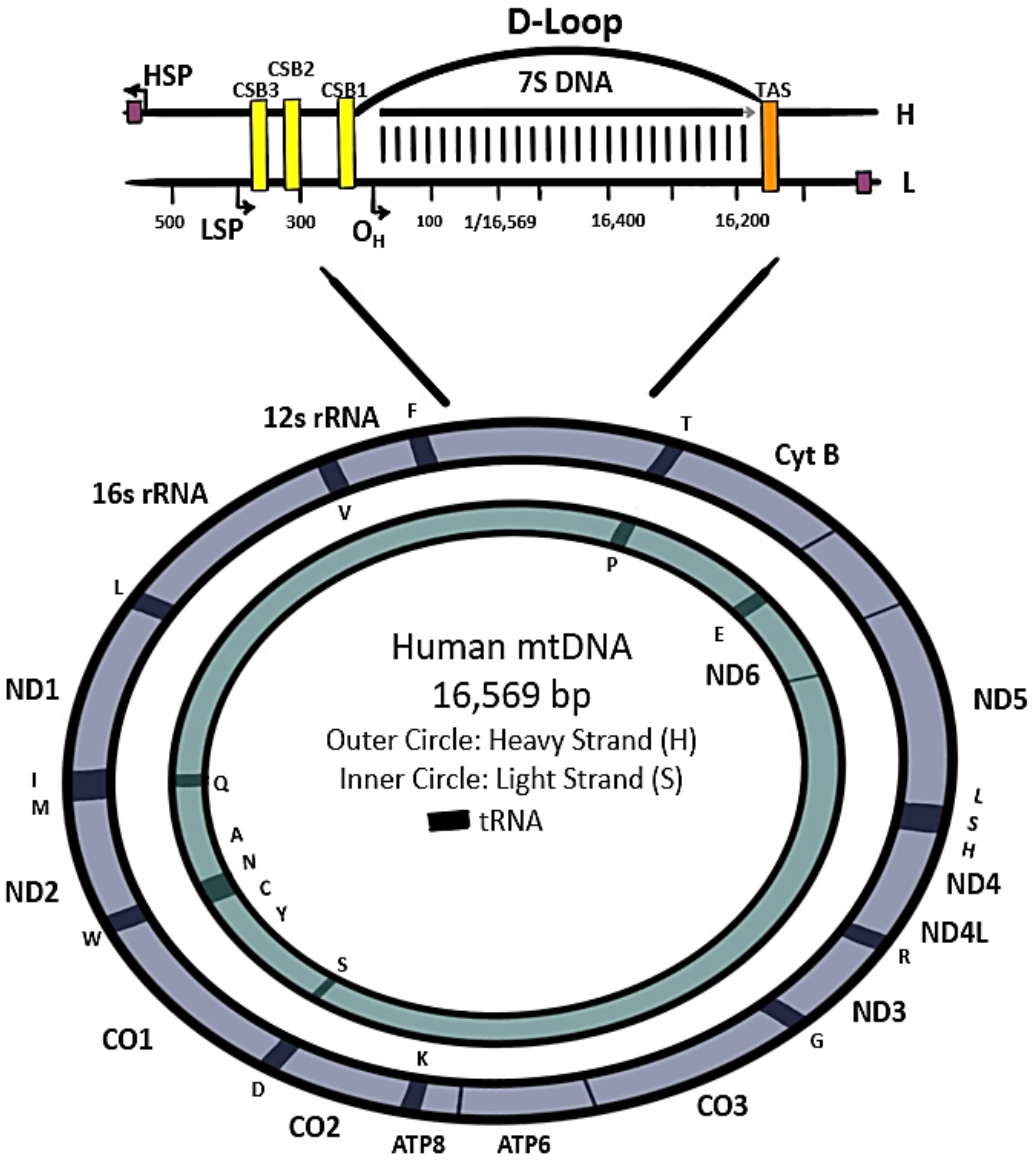

Figure 2. Human mitochondrial genome.

Mitochondrial genome is double-stranded: the heavy (H) strand (*the outer purple circle*) and the light (L) strand (*the inner blue circle*). It encodes 22 tRNAs (*dark strips*), 13 mRNAs and 2 rRNAs. It also contains a major noncoding region (D-loop) (*enlarged at the top panel*) which harbors promoters of the H-strand (HSP) and L-strand (LSP), the H-strand origin of replication (O_H), three conserved sequence blocks (CSB1, CSB2, CSB3) (*in yellow*) and the termination-associated sequence (TAS) (*in orange*). The short 7S DNA fragment is the result of premature termination of H-strand replication at TAS and forms the triple-stranded displacement loop structure.

Mammalian mtDNA is packaged into nucleoprotein complexes called nucleoids with an average size of ~ 100 nm in diameter to fit inside the mitochondria (Kukat et al., 2011). Nucleoids are attached to the mitochondrial inner membrane through their thin filaments and are not enveloped by a membrane that separate them from the mitochondrial matrix (Prachař, 2016). Unlike the nuclear chromatin, mitochondrial nucleoids have no histones. Human mitochondrial nucleoids are suggested to be organized into an inner core region containing mtDNA and mtDNA-binding proteins involved in transcription and replication and an outer peripheral region where RNA processing and translation take place (Bogenhagen, 2012; Bogenhagen, Wang, Shen, & Kobayashi, 2003). The anchoring of the D-loop to the inner mitochondrial membrane allows for interactions with those proteins facilitating the formation of nucleoids (Lee & Han, 2017). Therefore, mutations in this region can disrupt nucleoid structure and change the binding affinities for associated proteins. The main structural protein component of nucleoid is mitochondrial transcription factor A (TFAM) at a ratio of 1 subunit per 16-17 bp of mtDNA (Bogenhagen, 2012) and approximately 1.4 mtDNA molecule is estimated to be compacted per nucleoid in human cells (Kukat et al., 2011). TFAM appears to compact mtDNA through cross-strand binding and loop formation to form irregularly shaped and slightly elongated structures (Kukat et al., 2015). The mtDNA compaction level varies between more open mtDNA molecules and fully compacted nucleoids and it is heavily regulated by the TFAM to DNA ratio (Kaufman et al., 2007). Possibly, the different forms of nucleoids correspond to their accessibility for active replication and/or transcription. Farge et al. (2014) reported that the formation of long TFAM filaments on the DNA can prevent the melting by helicase TWINKLE and block the progression of transcription and replication machineries. Thus, changes in TFAM levels can have a regulatory effect on mtDNA copy number and gene expression.

1.1.4. Mitochondrial Transcription, Translation and Replication

Mitochondrial DNA expression and maintenance are complex processes involving various layers of regulation including mtDNA replication, mtDNA transcription, processing of RNA transcripts, RNA modifications, translation and positioning of the translated proteins into the inner mitochondrial membrane (Gustafsson, Falkenberg, & Larsson, 2016). Mitochondrial DNA is transcribed as long polycistronic transcripts and is initiated in the major noncoding region at HSP for the heavy strand and LSP for the light strand. The L-strand promoter is responsible for the transcription of *MTND6* and eight tRNAs, while the H-strand transcription is hypothesized (Montoya, Christianson, Levens, Rabinowitz, & Attardi, 1982) to be controlled by two promoters: HSP1 which generates a transcript containing $tRNA^{Phe}$, $tRNA^{Val}$, 12S rRNA and 16S rRNA and HSP2 which controls that transcription of almost the entire length of H-strand. The two-HSP-promoter model is still debated, and it was initially suggested in an attempt to justify the 50-fold increase in the steady state rRNAs levels compared to that of mRNAs. Mitochondrial DNA transcription machinery includes three main components: mitochondrial RNA polymerase (POLRMT), TFAM and mitochondrial transcription factor B2 (TFB2M). The transcription is initiated by the binding of TFAM to its binding site upstream the transcription start site inducing a 180° bend in the promoter DNA (Ngo, Kaiser, & Chan, 2011). Subsequently, POLRMT is recruited through its interactions with TFAM and DNA which is facilitated by the structural change (Yakubovskaya et al., 2014). Then, the initiation complex is fully formed when the POLRMT undergoes a conformational change allowing TFB2M's binding. Next, the mitochondrial transcription elongation factor forms a 'sliding clamp' around DNA downstream of POLRMT interacting with it and stimulating the transcription of long stretches of RNA (Hillen et al., 2017). Interestingly, L-strand transcripts are usually prematurely terminated at the conserved

sequence block 2 (CSB2) of the D-loop and it was proposed that the resulting short RNA serves as part of RNA to DNA transition sites for DNA replication (Xuan et al., 2006). However, the mitochondrial transcription elongation factor prevents the premature transcription termination of L-strand which can regulate the transition between replication and transcription (Agaronyan, Morozov, Anikin, & Temiakov, 2015). Lastly, the mitochondrial transcription termination factor 1 was identified as a main factor responsible for terminating transcription (Fernandez-Silva, Martinez-Azorin, Micol, & Attardi, 1997), however, the detailed mechanism of action remains unclear.

The primary RNA polycistronic transcripts undergo processing to produce the single RNA transcripts. The RNA processing event is believed to be predominately cotranscriptional considering the low steady state polycistronic RNA levels (Gustafsson et al., 2016). The tRNA punctuation model of RNA processing, proposed by Ojala, Montoya, and Attardi (1981), states that the release of single mRNA, rRNA and tRNA transcripts is achieved by the specific recognition and endonucleolytic cleavage of the flanking tRNAs at the 5'- and 3'- end by ribonuclease (RNase) P and Z, respectively (Hällberg & Larsson, 2014). Since not all mRNAs are flanked by tRNAs, another family of proteins were identified to play a role in RNA processing known as Fas-activated serine/threonine kinase (Jourdain et al., 2015). Following excision from the primary transcript, the separated transcripts will undergo maturation by polyadenylation, CAA addition and chemical modification (Hällberg & Larsson, 2014). With regards to mRNAs, polyadenylic acid RNA polymerase is responsible for catalyzing the 3' polyadenylation of all mRNAs, except *MTND6* and it was reported to exhibit a mRNA-specific effect (Tomecki, 2004). Moreover, leucine-rich penticopeptide rich domain containing protein is involved in controlling the stability of H-strand transcripts (Sterky, Ruzzenente, Gustafsson, Samuelsson, & Larsson,

2010) and is associated with poly (A) levels (Chujo et al., 2012). A study observed a loss of HSP transcripts and polyadenylation as well as transcriptional dysregulation in mice when leucine-rich penticopeptide rich domain containing protein was knocked out (Ruzzenente et al., 2012). It is important to note that a great number of noncoding RNAs complementary to mRNAs and rRNAs are generated during processing. Therefore, RNA degradation is essential for regulating the level of functional RNAs and the removal of processing by-products and aberrant RNA molecules (Borowski, Dziembowski, Hejnowicz, Stepien, & Szczesny, 2013). Both polynucleotide phosphorylase and human Suv3 protein helicase were identified to form a complex known as degradosome mediating RNA decay. In case of mitochondrial tRNAs, they are extensively altered during their maturation through chemical modifications and CCA addition (D'Souza & Minczuk, 2018). The tRNA nucleotides are chemically modified by a variety of enzymes to facilitate the codon recognition and interactions during translation. Then, tRNAs are coupled by aminoacyl tRNA-synthetases with their corresponding amino acids. Furthermore, mitoribosome maturation involves the chemical nucleotide modifications of rRNA and the import of many nuclear-encoded proteins needed for mitoribosome assembly. Mitoribosomes are quite unique in their composition as they contain numerous mitochondria-specific proteins as well as mitochondrial $tRNA^{Val}$ for structural support (Amunts, Brown, Toots, Scheres, & Ramakrishnan, 2015).

Although that the mitochondria contain their own ribosomes and tRNAs necessarily of DNA translation, mtDNA translation is entirely regulated by many nuclear-encoded proteins including mitochondrial translation initiation factors mtIF2 and mtIF3 (Gaur et al., 2008). mtIF3 inhibits the premature association of the large subunit with small subunit and places mRNA initiation codons (AUG/AUA) at the peptidyl site in the small subunit (Haque & Spremulli, 2008) while mtIF2, due to its increased affinity to the post transcriptionally modified initiator

formlymethionine tRNA, leads to the binding of formlymethionine tRNA to the cognate start codon of mRNA transcript (Spencer & Spremulli, 2004). During translation elongation, aminoacyl tRNA is guided to the large subunit's acceptor site to bind to its complementary codon with the help of the mitochondrial translation elongation factor Tu and guanosine triphosphate (D'Souza & Minczuk, 2018). Another factor known as elongation factor G 1 facilitates the exit of the deacetylated tRNA and the translocation of peptidyl tRNA within the mitoribosome (Hammarsund et al., 2001). The elongation step repeats itself until the stop codon is positioned in the acceptor site of the large subunit. Eventually, the stop codon (UAA/UAG) is recognized by the mitochondrial translation release factor 1a which catalyzes the release of peptidyl-tRNA from the acceptor site (Soleimanpour-Lichaei et al., 2007). Following that, the dissociation of mRNA, ribosomal subunits and deacetylated tRNAs are induced by the mitochondrial ribosomal recycling factor (Rorbach et al., 2008).

Replication of mtDNA is regulated by a number of nuclear-encoded, mitochondria-specific replication factors including DNA polymerase γ (POLγ), mitochondrial TWINKLE helicase and mitochondrial single-stranded DNA-binding protein (mtSSB) (Falkenberg, 2018). A model known as the strand-displacement model was proposed to explain the process of mtDNA replication in which no Okazaki fragments are synthesized and both strands are replicated continuously (Clayton, 1991). Replication is initiated from two different origins: O_H for H-strand and O_L for L-strand, however the H-strand synthesis is needed for the initiation of L-strand replication. The short transcripts generated from the premature termination of L-strand transcription are used as a primer by POLγ to initiate the H-strand replication at O_H (D. D. Chang & Clayton, 1985). TWINKLE travels downstream POLγ unwinding the double stranded DNA template while mtSSB binds to the newly formed single-stranded DNA protecting it from nuclease

digestion, secondary structure formation and random RNA synthesis by POLRMT (Miralles Fusté et al., 2014). As the helicase passes through O_L two-thirds down the genome, the H-strand forms a stem-loop structure at O_L preventing mtSSB from binding and permitting the initiation of ~25 bp primer RNA synthesis in the loop region (Fusté et al., 2010). Then, L-strand replication is initiated by POLγ and both strands' replications continue simultaneously. At the end of replication, the RNA primers are removed from the newly synthesized DNA strands by ribonuclease H1 (Cerritelli et al., 2003) and each of the new strands are then attached by DNA ligase III (Lakshmipathy & Campbell, 1999).

1.2. DNA Methylation

1.2.1. Mitochondrial DNA Methylation

Epigenetics refer to the reversible, inheritable modifications that regulate gene expression without any alterations in DNA sequence. These modifications include histone modifications, DNA methylation and noncoding RNAs and they regulate differential gene expression and biological processes in different cell types within an organism. DNA methylation is one of most extensively studied epigenetic modifications; however, mtDNA methylation has not been researched as extensively as methylation of nDNA despite the growing evidence of its existence. DNA methylation, the covalent addition of a methyl group from S-adenosylmethionine (SAM) to the cytosine base, is catalyzed by DNA methyltransferase enzymes (DNMTs) and results in the formation of 5-methylcytosine (5-mC). nDNA cytosine methylation is predominantly found in eukaryotes within cytosine-guanine dinucleotide (CpG)-rich regions. However, CpG islands, 500-1500 bp stretch of DNA with a G+C content $\geq$ 55%, are associated with some regulatory regions and generally unmethylated. Their methylation is mainly responsible for long-term silencing of genes such as imprinted genes. Unlike nDNA, mtDNA does not contain CpG Islands given its

small genome size. There are two classes of methyltransferases: the *de novo* methyltransferase DNMT3a and DNMT3b which establishes the methylation mark onto the unmethylated CpG region, and the maintenance methyltransferase DNMT1 which maintains the methylation through the addition of methyl group to hemi-methylated regions during replication (Lyko, 2018). Shock et al. (2011) discovered a mitochondrially targeted isoform of DNMT1 (mtDNMT1), which accounts for 1-2% of total DNMT1 transcripts, containing a targeted sequence upstream its transcription start site (TSS) which helps its translocation to the mitochondria. Hypoxia-responsive transcription factors such as peroxisome proliferator-activated receptor gamma coactivator 1 alpha and nuclear respiratory factor 1 were reported to be involved in the regulation of mtDNMT1 expression (Shock et al., 2011). Moreover, the presence of other DNMTs in the mitochondria was found to be inconsistent showing preference depending on the cell type (Bellizzi et al., 2013; Shock et al., 2011; Wong, Gertz, Chestnut, & Martin, 2013). For example, the localization of DNMT3a was identified to be in a tissue-specific manner and mainly occurs in the mitochondria of excitable tissues such as skeletal muscle, brain, heart and spinal cord (Wong et al., 2013).

Methylcytosine can be demethylated either passively through replication or actively through oxidation by ten-eleven translocation dioxygenase (TET) enzymes producing 5-hydroxymethylcytosine (5-hmC), which can be further oxidized to form 5-formylcytosine (5-fC) and then to 5-carboxylcytosine (5-caC) (X. Wu & Zhang, 2017). Active demethylation can also be through deamination by activation-induced deaminase/the apolipoprotein B mRNA editing enzyme catalytic polypeptide-like 3 (APOBEC3) (Bochtler, Kolano, & Xu, 2017). The active demethylation products can be then recognized and excised by thymidine DNA glycosylase followed by base excision repair to restore the unmodified cytosine base. TET enzymes were identified within the mitochondria via western blotting and immunofluorescence imaging (Bellizzi

et al., 2013; Dzitoyeva, Chen, & Manev, 2012),. Furthermore, the recent detection of APOBEC3 in the mitochondria (Wakae et al., 2018) suggests that mtDNA might undergo active cytosine demethylation through both the deamination by APOBEC3 as well as the oxidation by TET enzymes.

Despite the increasing interest in mtDNA methylation over the last decade, its function has not been fully comprehended yet. In an attempt to understand the functional capacity of mtDNA methylation, a group used mitochondria-targeted bacterial CpG methyltransferase (M.SssI) and Chlorella virus GpC methyltransferase (M.CviPI) to induce methylation and reported that an increase in GpC methylation reduced the HSP-regulated mtDNA transcription; thus, implying that mtDNA methylation in the GpC context might be the one controlling gene expression as opposed to CpG methylation (Van Der Wijst, Van Tilburg, Ruiters, & Rots, 2017). However, this study induced methylation to far beyond the previously estimated endogenous levels and its physiological relevance needs to be further evaluated. Additionally, the upregulation of mtDNMT1 was found to correlate with non-random, both gene- and strand-specific changes in mitochondrial gene expression such as the activation of HSP-regulated *MTND1* and repression of LSP-regulated *MTND6,* while *MTCO1* and *MTATP6* remained unaffected (Shock et al., 2011). Moreover, the mtDNA methylation within the non-coding D-loop region drew more attention than other regions due to its biological importance in regulating mtDNA replication and transcription as it contains promoters HSP and LSP as well as origin of replication O_H, therefore its methylation is believed to potentially play a role in influencing these process in the mitochondria (Bellizzi et al., 2013; Van Der Wijst et al., 2017).

Beside CpG methylation, studies in their efforts to widely explore mtDNA methylation have identified both non-CpG and adenine methylation in the mitochondrial genome. Patil et al.

(2019) used whole genome bisulfite sequencing in liver and breast cell lines and observed that mtDNA is heavily methylated (around 30%) in a predominantly non-CpG context (CpC, CpT, CpA) with CpG sites having the lowest methylation levels. Moreover, adenine base can be methylated resulting in N^6-methyladenine (6-mA). Although adenine methylation is mostly common in prokaryotes where it is used to help the organism distinguish foreign DNA from self-DNA and eliminate it, it was found to be present in higher eukaryotes including humans (Xiao et al., 2018). Koh et al. (2018) reported that mtDNA has > 8,000 times more 6-mAs than nDNA, primarily enriched in the heavy strand. It was associated with the regulation of mtDNA replication through promoting the melting of double-stranded mtDNA and the recruitment of mtSSB which was identified as a putative 6-mA binding protein. The adenine methylation machinery has not been fully recognized yet in the mitochondria; however, the enzyme ALKBH1 catalyzing the demethylation of methyladenine was identified.

1.2.2. DNA Methylation Detection Methods

There are several methods to detect both genome-wide and locus-specific DNA methylation (Barros-Silva, Marques, Henrique, & Jerónimo, 2018). There are restriction enzymes-based methods which are used to identify methylation at single base resolution using both methyl-sensitive and insensitive enzymes for restriction digestion; however, not all cytosines are covered, especially in regions that do not contain the enzyme restriction site. Then, there are the bisulfite conversion-based methods which are based on the sodium bisulfite treatment of DNA leading to the conversion of unmodified cytosines into uracil while 5-mC remain unchanged (Frommer et al., 1992). This technique allows the methylation of all the cytosines in different contexts to be evaluated at high resolution; however, it is highly priced and requires high DNA input as a considerable amount of input is lost due to the strong conditions that the DNA is subjected to

during bisulfite treatment. It should be noted that bisulfite conversion does not discriminate between 5-mC and 5-hmC and in order to overcome this issue, two methods have been produced: oxidative bisulfite sequencing (oxBS-seq) (Booth et al., 2012) and TET-assisted bisulfite sequencing (TAB-seq) (Yu et al., 2012). In oxBS-seq, potassium perruthenate is used to oxidize 5-hmC to 5-fC while leaving unmodified cytosine and 5-mC unchanged (Booth et al., 2012). The differences between 5-hmC and 5-mC is demonstrated when bisulfite converts 5-fC and unmodified cytosine to uracil and leaves 5-mC unchanged. Alternatively, TAB-seq uses TET enzyme to oxidize 5-mC to 5-caC after attaching a glucose molecule to 5-hmC using β-glucosyltransferase to create β-glucosyl-5-methylcytosine (5-gmC) (Yu et al., 2012). During bisulfite conversion, unmodified cytosine and 5-caC are converted to uracil and 5-carboxyluracil respectively, but the 5-hmC remains modified as 5-gmC. Another approach for methylation detection is the affinity enrichment-based methods which involve purification of the methylated DNA fragments following sonication and incubation with either a methyl-CpG binding domain (MBD-seq) (Serre, Lee, & Ting, 2010) or a 5-mC antibody (methylated DNA immunoprecipitation sequencing (MeDIP-seq)) (Mohn, Weber, Schübeler, & Roloff, 2009). MBD-seq and MeDIP-seq are both cost-effective methods and differentiate between 5-mC and 5-hmC. However, they have lower resolution of a ~150 bp window. Moreover, MBD-seq is biased toward hypermethylated and CpG dense regions. Therefore, non-CpGs and less dense CpG areas may not be covered. Despite MeDIP-seq also being biased towards hypermethylated regions, it can, by contrast detect cytosine methylation irrespective of context (CpG and non-CpG) and its accuracy depends primarily on the specificity and sensitivity of the chosen antibody to avoid nonspecific binding.

A technical limitation of bisulfite treatment was raised by Liu et al. (2016) when comparing the methylation levels of mtDNA in its circular structure with that of linearized structure. They

concluded that the CpG methylation is a rare event in the mitochondria as the average methylation of 83 CpG sites across 9 regions of mtDNA was below 2%. The circular structure of mtDNA was observed to cause an overestimation of the methylation values due to the inefficient bisulfite conversion and they recommended mtDNA linearization before using bisulfite-based method. However, it should be noted that the experimental conditions, such as template purity, primer quality and amplification success, under which methylation is analyzed by bisulfite-based methods also have a major role to play in determining the accuracy of methylation data (Owa, Poulin, Yan, & Shioda, 2018). Moreover, nuclear DNA sequences of mitochondrial origin (NUMTs), which are nuclear regions that have high-sequence homology with mtDNA (Woischnik & Moraes, 2002) is another possible factor that can lead to false positive methylation values of mitochondrial genome.

1.2.3. Mitochondrial DNA Methylation Conundrum

There has been a lot of controversy surrounding mtDNA methylation since it was first reported almost five decades ago. One of the earliest studies by Nass (1973) showed that mtDNA methylation exists in mouse and hamster cell lines and is significantly less than that of nDNA when measured using radioactive labelling. Subsequently, Shmookler Reis & Goldstein (1983) reported that 2-5% of mtDNA was fully methylated at the specific restriction site (-CCGG-) regions in human fibroblast cells when analyzed by Southern blot hybridization after digestion with methylation-sensitive restriction enzymes. Additionally, mitochondrial methylation was studied by Pollack, Kasir, Shemer, Metzger, and Szyf (1984) in mouse by restriction digestion techniques and found it to be a nonrandom event with very low CpG methylation levels of 3 - 5%. Later, mtDNA methylation continued to be detected via different methods in various cell types such as mouse brain tissue using enzyme-linked immunosorbent assay (Dzitoyeva et al., 2012), human colorectal cancer cells (Shock et al., 2011) and brain tissue (Devall et al., 2017) using

MeDIP and human blood cells by bisulfite sequencing (Bellizzi et al., 2013). Furthermore, several reports in mouse and human have assessed mtDNA methylation levels to range from 2% to 18% in D-loop or 12 rRNA or 16S rRNA (H.-M. Byun et al., 2013; H. M. Byun & Barrow, 2015; B. G. Janssen et al., 2014; Wong et al., 2013). Despite these findings and many others supporting the presence of mtDNA methylation in the D-loop and several mitochondrial genes, it remains debated and studies continue to report its absence and/or the lack of its biological significance given the very low level detected (Hong, Okitsu, Smith, & Hsieh, 2013; Mechta, Ingerslev, Fabre, Picard, & Barrès, 2017).

1.2.4. Factors Affecting Mitochondrial DNA Methylation

With the potential role of mitochondrial methylation in the mtDNA regulation, aberrant methylation patterns may, therefore, result in mitochondrial dysfunction and increased risk of disease. The epigenetic patterns, especially of DNA methylation, can be impacted by a variety of external factors such as environmental exposures, pharmaceutical drugs and diet particularly in early life. Maternal diet has been consistently shown to alter nDNA methylation of offspring in both human cord and peripheral blood which may predict their health later in life (James et al., 2018). Micronutrients in the diet such as folate, methionine, chlorine, vitamin B6 and vitamin B12 influence methylation through mediating the one-carbon metabolism pathways and maintaining SAM levels (O. S. Anderson, Sant, & Dolinoy, 2012). The methyl-tetrahydrofolate is used to donate a methyl group for the formation of methionine from homocysteine. Then, methionine is converted to SAM which serves as the major methyl donor for DNMT-catalyzed methylation of cytosine. Interestingly, Jia et al. (2015) showed that maternal nutrition during pregnancy could also impact mtDNA methylation where maternal betaine (a product of chlorine degradation) supplementation throughout pregnancy reduced D-loop methylation enhancing the mitochondrial

gene expression including *MTND5*, *MTCO1* and *MTCO2* in offspring piglets' skeletal muscles. Moreover, the effect of high- and low-lipid diet on mtDNA methylation was examined in the liver of large yellow croaker fish (Liao, Yan, Mai, & Ai, 2016). While a significant increase in D-loop methylation among the high-lipid diet group compared to controls was observed without any changes in gene expression, the low-lipid diet group showed an increase in mtDNA copy number as well as an upregulation of *MTCO1*, *MTCO2*, *MTATP6*, *MTRNR1*, and *MTRNR2* which might be a form of adaptive metabolic mechanisms for ATP production in response to low-lipid diet.

Exposure to smoking and air pollution is reported to induce changes in methylation which can underlie the increased risk of disease. A study aiming to investigate the effect of maternal smoking during pregnancy on mtDNA methylation in a birth cohort reported an increased methylation D-loop region of the placental and neonatal tissue; however, whether these differences have an impact on fetal development or long-term health is not well known (Armstrong et al., 2016). Moreover, similar placental mtDNA methylation changes were found in the D-loop as well as *MTRNR1* of pregnant women exposed to air pollution in the form of $PM_{2.5}$ airborne particulate matter (< 2.5 μm diameter) which might mediate the observed decrease in placental mtDNA content (Bram G. Janssen et al., 2015). Byun et al. (2013) has tested the sensitivity of peripheral blood mtDNA methylation to three airborne pollutants and reported that steel workers who were exposed to high metal-rich particulate matter exposure showed increased methylation in *MTRNR1* and *MTTF* than low-exposed controls, while traffic-derived Elemental Carbon and air benzene did not have any effect on mtDNA methylation. In contrast, metal exposure, such as arsenic and chromium via water pollution or workplace was found to be associated with a decrease in the mtDNA methylation of several mitochondrial genes including D-loop and *MTND6* (Sanyal,

Bhattacharjee, Bhattacharjee, & Bhattacharjee, 2018) as well as *MTTF* and *MTRNR1* (Linqing et al., 2016).

Pharmaceutical drugs are another factor that was examined in several studies as the altered mtDNA methylation in patients might be the underlying cause for drug-induced mitochondrial pathogenesis. For example, valproic acid is an anticonvulsant drug commonly used for epilepsy treatment and seizure management and may lead to liver toxicity and steatosis (Silva et al., 2008). In a study, primary human hepatocytes were treated with valproic acid and the MeDIP-seq results suggested a potential crosstalk between the nucleus and mitochondria. The reduction in methylation of seven mtDNA genes, including *MTCO1* and *MTCO2*, was concurrent with the hypermethylation of nuclear DNA-encoded DNMT and methionine adenosyltransferase , the enzyme catalyzing the production of SAM (Wolters et al., 2017). *MTCO1*and *MTCO2* encode for cytochrome c oxidase subunits comprising complex IV of the electron transport chain and one of the major sites for reactive oxygen species formation (Cadenas & Davies, 2000). Hence, its dysregulation promotes the release of reactive oxygen species and induces oxidative stress which might be the cause of liver toxicity.

CHAPTER TWO

2.0 RATIONALE, HYPOTHESIS AND RESEARCH AIMS

2.1. Rationale

DNA methylation is a key epigenetic modification involved in gene regulation and predominately found in the nuclear genome of various organisms. Interestingly, mtDNA has also been found to be modified by 5-mC and it is receiving an increasing interest, particularly in diseases characterized by mitochondrial dysfunction such as neurodegenerative diseases (Wong et al., 2013) and Diabetes Mellitus (Mishra & Kowluru, 2015). However, more understanding of the interindividual methylation variation, especially that of the mitochondrial genome, in the normal physiological state is needed. This knowledge is integral in understanding what arises during the pathological state and most importantly needed to control for basal background in analyses involving exposure-associated DNA methylation differences.

Peripheral blood leukocytes are the most frequently used cell types to monitor changes in their nDNA methylation in response to disease (Di Francesco et al., 2015; Javierre et al., 2010). They are easily accessible, and reflective of the individual's systemic health state as they communicate and exchange signals with all the peripheral tissues through their receptor binding to numerous signaling molecules. Therefore, the variation in their mitochondrial methylation status could potentially be useful as an indicator of the physiological status in future diagnostic tools.

Most studies of DNA methylation in blood involve the isolation and analysis of total leukocytes with mixed cellular populations (Terry, Delgado-Cruzata, Vin-Raviv, Wu, & Santella, 2011). Different leukocytes with distinct functions exhibit differential gene expression which could be accounted for by the differential DNA methylation within cell types in individual samples (H. C. Wu et al., 2011). Thus, it would be challenging to interpret results and distinguish between

changes in methylation that are due to health or environmental conditions and those resulting from the cellular population heterogeneity in blood samples which raises the importance of cell type purification (H. C. Wu et al., 2011). Moreover, Hohos et al. (2016) showed that different classes of leukocytes differentially regulate nDNA methylation where $CD4^+$ helper T cells and CD8+ cytotoxic T cells found to be the "most distinctly poised for rapid methylome response to physiological stress and disease", with $CD8^+$ T cells having elevated levels of 5-mC relative to other peripheral blood mononuclear cells (PBMCs). Therefore, for the study being proposed, circulating $CD4^+$ and $CD8^+$ T cells collected from healthy individuals are used as a study model to investigate the basal mitochondrial methylation of these specific cell types. Knowing the extent of these variations in the healthy individuals is needed to understand perturbations in DNA patterns that are a consequence of altered physiological states.

2.2. Hypothesis

There are variations in the mtDNA methylation patterns in both $CD4^+$ and $CD8^+$ T cells among individuals.

2.3. Research Aims

2.3.1. Aim 1: Determining the mtDNA methylation patterns of $CD4^+$ and $CD8^+$ T cells from healthy individuals.

In order to analyze the mtDNA methylation of $CD4^+$ and $CD8^+$ T cells, blood samples of ten self-declared healthy individuals will be collected and PBMCs will be separated through density gradient centrifugation. The samples will be then sorted into $CD4^+$ and $CD8^+$ T cells by immunomagnetic negative selection to avoid any possible activation of these cells. The isolated genomic DNA (gDNA) will be sonicated, and the methylated fragments will be pulled down by MBD-coupled magnetic beads. Subsequently, the eluted DNA samples will be sequenced and the

mtDNA methylation data analysis will be performed by the bioinformatician Dr. Tobias Karakach. Finally, the methylation level of CpG sites within the mitochondrial D-loop control region will be quantitatively measured by bisulfite pyrosequencing to get a sense of the degree of methylation in mtDNA.

2.3.2. Aim 2: Determining the effect of the mitochondrial/nuclear DNA ratio on the mtDNA methylation in $CD4^+$ and $CD8^+$ T cells.

mtDNA cellular content differs across tissue types depending on several factors including the cellular energy demand which influence various mitochondrial processes. By estimating the mitochondrial/nuclear DNA ratio, we get an idea of the relative amount of mtDNA and whether the mtDNA cellular content could possibly be linked to the mtDNA methylation patterns detected in a cell type. Quantitative PCR (qPCR) will be performed using nuclear primer for glyceraldehyde 3-phosphate dehydrogenase (*GAPDH*) and mitochondrial primer for cytochrome B (*MTCYB*) to measure the mitochondrial/nuclear DNA ratio in $CD4^+$ and $CD8^+$ T cells.

CHAPTER THREE

3.0 MATERIALS AND METHODS

3.1. Blood Sample Collection and $CD4^+$ and $CD8^+$ T Cells Isolation

Ten nonfasted, self-declared healthy participants free from infectious diseases were recruited. The University of Manitoba Biomedical Research Ethics Board approved the study and all study participants provided written informed consent after being made aware of the design of the study. Venous whole blood samples (10 ml each) were collected in ethylenediaminetetraacetic acid (EDTA) coated tubes (BD Vacutainer®). Peripheral blood mononuclear cells were isolated by centrifugation at 800 x g for 20 minutes at room temperature over a density gradient medium (Lymphoprep™, STEMCELL). PBMCs were then sorted into purified $CD4^+$ and $CD8^+$ T cells and a fraction of unsorted PBMCs for analyses of 5-mC. The T cells were isolated using EasySep™ Human $CD4^+$ T Cell Enrichment and EasySep™ Human $CD8^+$ T Cell Enrichment Kits (STEMCELL) as per the manufacturer's instructions. The purity of isolation was checked by flow cytometry. The isolation protocol was based on immunomagnetic negative selection where unwanted cells were pulled down by a mixture of antibody-magnetic complexes while cells of interest remained free in the supernatant to avoid their activation or any changes in their nature. The blood collection and mononuclear cells isolation were performed by Dr. Ruey-Chyi Su's lab at the JC Wilt Infectious Diseases Research Centre.

3.2. Total Genomic DNA Extraction

Total gDNA was purified from the $CD4^+$ T cells, $CD8^+$ T cells, and PBMCs by using QIAamp DNA Mini Kit (Qiagen) as per the manufacturer's instructions. The DNA was eluted in 200 µl of the provided elution buffer and stored at -20°C. The concentrations of eluted DNA were measured by using the Qubit 2.0 Fluorometer (Life Technologies).

3.3. Isolation of Methylated DNA by MethylMiner

3.3.1. Validation of MethylMiner Kit

The MethylMiner Methylated DNA Enrichment Kit (Invitrogen) was used to pull down the methylated DNA fragments. The use of MethylMiner kit was validated prior to running the experiment on the study samples. Two 80 bp-long synthetic methylated and non-methylated duplex DNAs (1 ng/µl) and pre-fragmented DNA from cultured K-562 cells (50 µg/ml) were included in the kit to be used as controls in an external control reaction. The methylated synthetic duplex was used as a positive control containing 8 fully methylated CpG sites along its length whereas the non-methylated duplex was used as a negative control with 9 non-methylated CpG sites along its length. The synthetic duplexes were diluted to 10 pg/µl, and 10 pg of each diluted duplex DNA was spiked into 1µg of the K-562 DNA control sample in 20 µl of 5X Wash / Bind buffer. The control sample mixture was brought up to a total volume of 100 µl with DNase-free water. Coupling of 7 µl (3.5 µg) of MBD-Biotin Protein to 10 µl of Dynabeads M-280 Streptavidin was done according to the manufacturer's instructions through a series of washes with 1X Wash / Bind buffer and a one-hour rotation at room temperature. Then, the MBD-Biotin-Streptavidin beads were washed three times with 5-minute rotation each and resuspended in 100 µl of 1X Wash / Bind buffer before adding it to the control sample mixture for the capture reaction. The capture reaction was performed by incubation with the MBD-coupled magnetic beads on a rotating mixer for an hour at room temperature. The beads in capture reaction tube were washed three times afterwards with 1X Wash / Bind buffer and 3-minute rotation each, and the captured methylated DNA fragments were eluted twice as a single fraction with 200 µl of high-salt elution buffer (2000 mM NaCl). The fraction was precipitated using two sample volumes (800 µl) of 100% ethanol, 1 µl glycogen (20 µg/µl) and one-tenth sample volume (40 µl) of 3 M sodium acetate (pH 5.2)

followed by two-hour incubation at – 80°C and a series of centrifugation steps. Finally, the methylated DNA pellet was resuspended in 60 µl 1X TE buffer (10 mM Tris-HCL pH 7.5 and 1 mM EDTA) and stored at -20 °C.

Endpoint PCR was performed to detect the eluted methylated DNA fragments following the control capture reaction. The control sample mixture (input), the collected supernatant following the incubation with beads (unbound) and the eluted DNA were amplified using the PCR primer sets provided in the kit which are specific for each synthetic duplex. Both the pre-fragmented K-562 DNA and a mixed DNA sample of diluted non-methylated and methylated synthetic duplexes were also included in the PCR. The PCR reactions were prepared in 0.2 ml tubes to a total volume of 20 µl by adding 1 µl of each DNA, 10 µl of the SYBR green master mix (Bio-Rad), 2 µl of primer mix (10 µM) and 7 µl of RNase free water (Thermo Fisher Scientific). The thermocycling conditions for PCR were as follows: 94°C for 2 minutes, 27 cycles of 94°C for 15 seconds, 55°C for 15 seconds and 68°C for 30 seconds, followed by 68°C for 5 minutes and 4°C hold. Subsequently, twenty percent of the resulting amplicons were loaded onto a 4% agarose gel with a 50 bp DNA ladder (Thermo Fisher Scientific). The agarose gel was prepared by dissolving 2 g of agarose (Invitrogen) in 50 ml 1X TBE buffer (100 mM Tris base, 100 mM Boric acid and 2 mM EDTA, pH 8.3) and heating it for 2 minutes in the microwave. Then, 10 µl of 1X GelStar nucleic acid gel stain (Lonza) was added to the liquid agarose once it cooled down. The gel was cast, left to solidify, and placed in 1X TBE buffer as the running buffer for the agarose gel electrophoresis. A 6X DNA gel loading dye (Thermo Fisher Scientific) was added to each amplicon sample before loading them and running the gel for 45 minutes at 150V. The gel was then removed to be viewed using GelDoc-it2 Imager (UVP). Once the kit was validated, MethylMiner was performed on test samples.

3.3.2. Isolation of Methylated DNA from Study Samples by MethylMiner

One microgram of gDNA of $CD4^+$ T cells, $CD8^+$ T cells, and PBMCs isolated from each of the 10 participants was sonicated to ~250-bp fragments using the Covaris S220 System in a 120 µl total volume with 1x low TE buffer (10 mM Tris-HCl, pH 8.0, 0.1 mM EDTA). The sonicated gDNA mixture was prepared by mixing 1 µg of sonicated gDNA with 20 µl of 5X Wash / Bind buffer and bringing the volume to 100 µl with DNase-free water. The capture reaction was performed (as described previously in section 3.3.1) and the methylated DNA pellet was resuspended in 60 µl 1X TE buffer and stored at -20 °C.

3.4. Library preparation

The quantity of methylated DNA fragments was measured using the Qubit 2.0 Fluorometer (Life Technologies). The quality and size of methylated DNA were checked using the Bioanalyzer (Agilent Technologies). Twenty nanogram of methylated DNA was used, and the libraries were prepared with the NEB Ultra II DNA Library Prep Kit according to the manufacturer's instructions. Both the quality check and library preparation were done by Ifeoluwa Adewumi of the Manitoba Next Generation Sequencing Platform. The samples were sent to Genome Quebec for sequencing by the Illumina HiSeq 4000 PE 100 sequencer with the depth of 33 million reads per sample. The bioinformatics data analysis was done, as shown below in **Figure 3**, by Dr. Tobias Karakach, a bioinformatician at the Children's Hospital Research Institute of Manitoba. The analysis involved preprocessing of the raw data, alignment of reads to the human mitochondrial genome from Human Genome Assembly GRCh37 (hg19), and methylation peak calling.

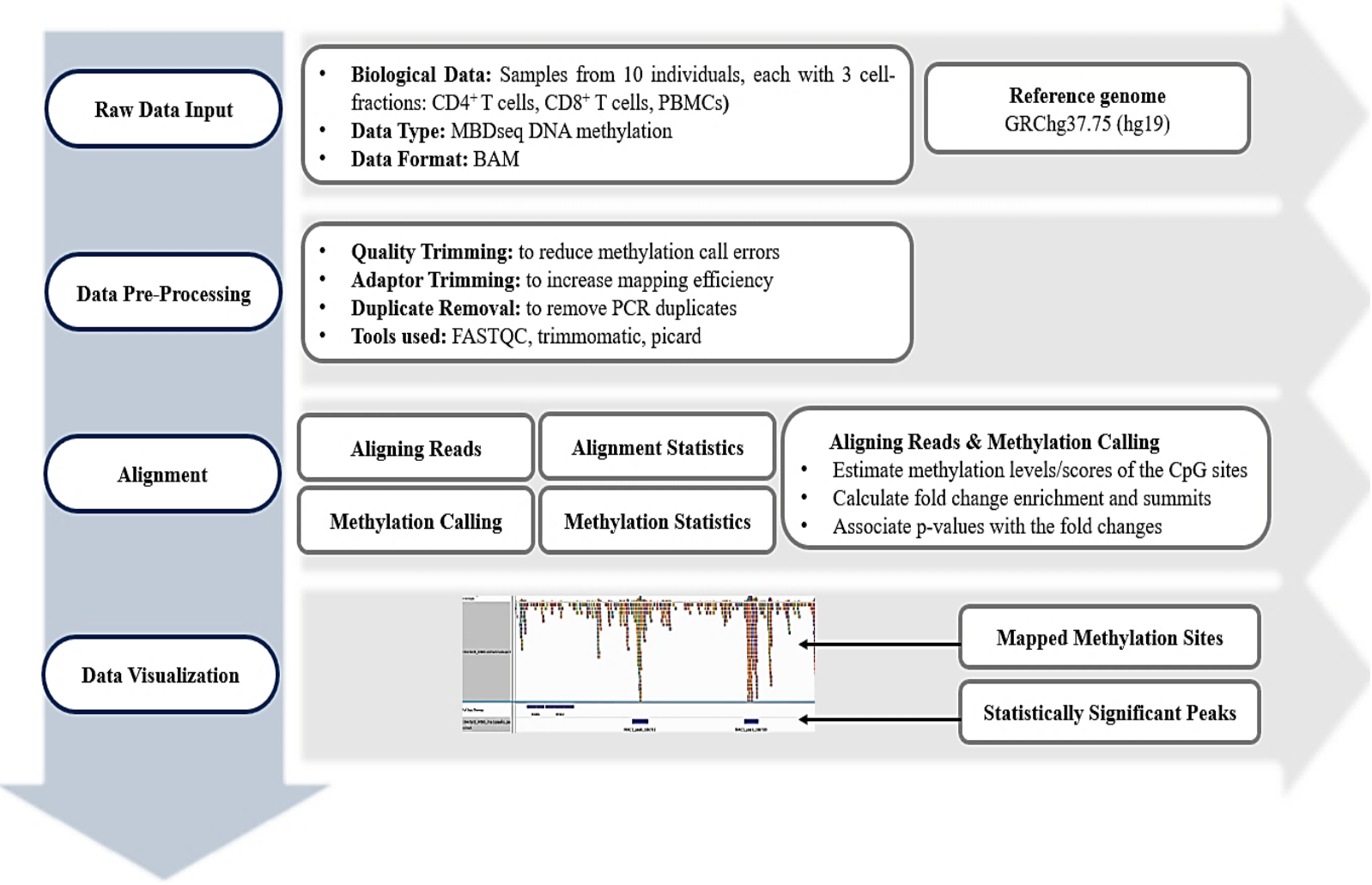

Figure 3. Workflow of the bioinformatic analysis pipeline.

3.5. DNA Methylation Analysis using Bisulfite -Pyrosequencing

Bisulfite-Pyrosequencing was used to quantitively estimate methylation levels at 6 CpG sites within the mitochondrial D-loop region of $CD4^+$ and $CD8^+$ T cells from 10 participants with the help of Dr. Jones lab in the Department of Biochemistry and Medical Genetics. Pyromark Assay Design Software 2.0 (Qiagen) was used to design bisulfite-pyrosequencing assays and generate the forward, reverse, and sequencing primers. Primer sequences are listed in **Table *1*** and their location is shown in **Figure 4**. Genomic DNA (200-500 ng) was bisulfite-converted using the EZ DNA Methylation Kit (Zymo Research) as per manufacture's protocol. The eluted bisulfite-converted DNA samples were quantified by NanoDrop 2000 (Thermo Fisher Scientific) and then diluted down to 15 ng/µl for PCR amplification. The region of interest was amplified by PCR with the forward biotinylated primer and reverse primer using the HotStar Taq DNA Polymerase Kit (Qiagen). The PCR reaction conditions used were as follows: 95°C for 15 minutes, 45 cycles of 95°C for 30 seconds, 58°C for 30 seconds, and 72°C for 30 seconds, then 72°C for 5 minutes. The PCR products (243 bp) were then examined by agarose gel electrophoresis. They were loaded onto a 1.5 % (1.5 g of agarose in 100 ml 1X TBE buffer) agarose gel with a 100 bp DNA ladder (GeneDireX) and viewed using GelDoc-it2 Imager (UVP). Next, the biotinylated PCR products were then immobilized on streptavidin-coated Sepharose beads (Streptavidin Sepharose High Performance, GE Healthcare) and prepared into a single-stranded DNA and released into the PyroMark Q96 HS Plate (Qiagen) using the PyroMark Vacuum Prep Workstation (Qiagen). The sequencing was done on the PyroMark Q96 MD Pyrosequencer (Qiagen) and the percent methylation at each of the targeted CpG sites of interest was calculated with the Pyro Q-CpG software (Qiagen) by measuring the relative peak height of T

versus C at a given CpG site. For bisulfite-conversion efficiency and quality control, Human Methylated and Non-methylated DNA Set (Zymo Research) was used to prepare a range of 0%, 25%, 50%, 75%, and 100% methylated sample controls for a standard curve and were included on each assay plate. Graphs were generated with R Statistical Software.

Table 1. List of the primers for the CpG sites in the mitochondrial D-loop region for pyrosequencing.

Region	CpG Location	PCR Primers	Amplicon Size (bp)	Sequencing Primers
D-loop	Six CpG sites: 16328, 16360, 16411, 16427, 16449, 16454	**Forward**: 5'-Biotin- GTT TTA TGA TTT TGA AGT AGG AAT TAG ATG-3'	**243 bp**	**1. Sequencing of two CpG sites (16328, 16360):** 5'-ACA TAA TAC ATA AAA CCA TTT ACC -3'
		Reverse: 5'-ACC TAC CCA CCC TTA ACA AT -3'		**2. Sequencing of four CpG sites (16411, 16427, 16449, 16454):** 5'- CTT AAC CAC CAT CCT -3'

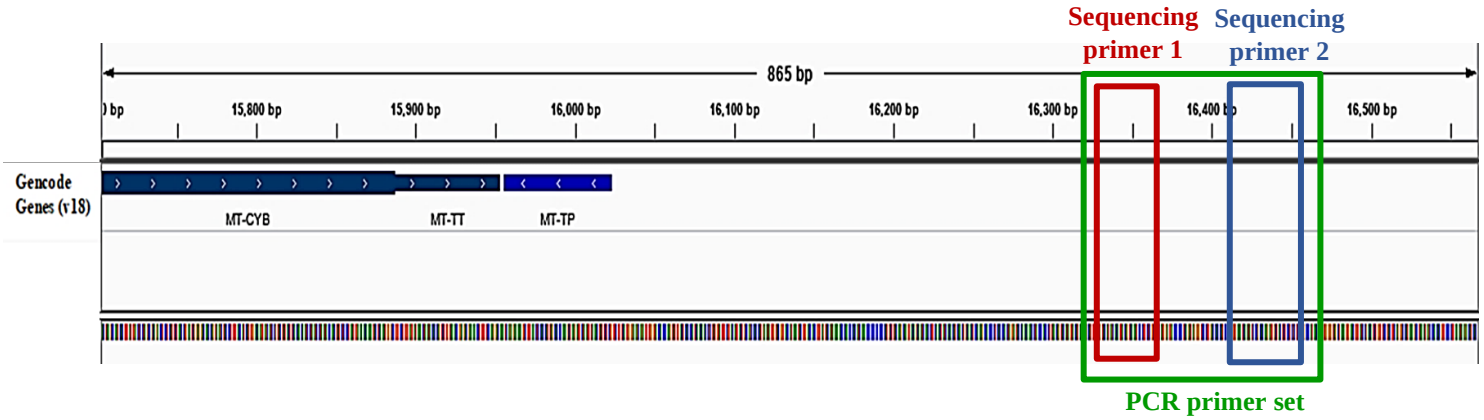

Figure 4. Location of the primers for pyrosequencing of six CpG sites within the mitochondrial D-loop.

The green box shows the location of the region (16321-16460 bp) amplified by the biotinylated PCR primer set. Sequencing primer 1 (red box) and sequencing primer 2 (blue box) correspond to regions that were pyrosequenced covering two CpG sites (16328, 16360) and four CpG sites (16411, 16427, 16449, 16454), respectively as shown in the Integrative Genomics Viewer (IGV) software.

3.6. Cell Culture

3.6.3. Cell Culture Conditions

The human embryonic kidney HEK293T cell line was obtained from the American Type Culture Collection (ATCC). The cells were grown in Dulbecco's Modified Eagle's Medium (DMEM) (Gibco®) inside 37°C incubator containing 5% carbon dioxide (CO_2). The base medium was supplemented with 10% Fetal Bovine Serum (FBS) and 1% Antibiotic-Antimycotic (Gibco®) at a pH of 7.2. The cells obtained for experiments in this study were at passage number 24.

3.6.4. Cell Passaging

Once the cells reached a confluency of 70-80%, they were subcultured. The culture medium was removed from the cell culture plate and discarded. Then, 1X sterile Phosphate Buffered Saline (PBS) was added to wash the cell monolayer and remove any traces of FBS which contains trypsin inhibitor. Following that, 1-4 ml of TrypLE Express Enzyme (Gibco®) was added depending on the size of the plate and cells were placed back in the 37°C incubator for 2-5 minutes until the cell layer was dispersed. To deactivate the enzyme, double its volume of growth medium was added and the detached cells were collected in a 15 ml centrifuge tube (Corning™ Falcon™). The cells were centrifuged at 300 x g for 3 minutes, and the cell pellet was resuspended in an appropriate volume of medium. The cell suspension was then aliquoted into new culture plates.

3.6.5. Cell Storage and Recovery

For cell cryopreservation, cells were cultured to 70-90% confluency. They were then washed with 1X sterile PBS and detached using TrypLE Express Enzyme. The cell suspension was collected in growth medium and the cell count and their viability were assessed using the TC20™ Automated Cell Counter (Bio-Rad) and Trypan Blue Stain (1:1) (Sigma). Afterwards, the cells were centrifuged at 300 x g for 3 minutes, and the cell pellet was resuspended in a freezing

medium composed of 95 % (v/v) DMEM with 5% (v/v) dimethyl sulfoxide (DMSO) (Sigma). The cells ($\geq 3 \times 10^6$ cells/ml) were aliquoted into cryovials (Thermo Fisher Scientific), labeled and stored in a -80°C freezer or a liquid nitrogen tank for long-term storage.

For cell revival, the cryovials of frozen cells were placed in a 37°C water bath until the cells were mostly thawed. The surface of vials was then decontaminated with 70% ethanol and the cells were transferred into a 15 ml centrifuge tube containing 5 ml DMEM and centrifuged at 300 x g for 3 minutes. The supernatant (media and DMSO) was discarded, and the cell pellet was transferred in 5 mL growth medium to 100 mm cell culture plates. The cells were allowed to adhere to the plate through overnight incubation at 37°C and medium was replaced by a fresh one the following day. The cells were checked daily until they reached the required confluency for passaging. The cells needed to be passaged a minimum of three times before being used for experiments.

3.7. Nuclear DNA Extraction

HEK293T cells were cultured to 70-80 % confluency. The medium was removed, and the cells were washed twice with ice cold 1X PBS, then collected by centrifugation at 6200 x g for 5 minutes at 4°C. Cells (5×10^6) were resuspended in a 15 ml centrifuge tube with 5 ml cell lysis buffer (5 mM PIPES (pH 8 with KOH), 85 mM KCl, 0.5% NP-40) supplemented with protease inhibitors. The cells were incubated for 10 minutes at 4°C with rotation. The cell suspension was then passed through a syringe with a 22-guage needle 10 times, then centrifuged at 2000 x g for 5 minutes at 4°C to obtain the nuclei. The nuclear pellet was resuspended and lysed with 0.5% sodium dodecyl sulfate (SDS) in MNase digestion buffer (10 mM Tris-HCl pH 7.5, 0.25 M sucrose, 75 mM NaCl) for an hour rotation at room temperature. The sample was then centrifuged at 13,000 rpm for 10 minutes at room temperature. The supernatant was treated with RNase A

(0.02 µg/ml final concentration for 30 minutes at 37°C) and Proteinase K (0.5 µg/ml final concentration for 1 hour at 55°C). Finally, the nuclear DNA was purified using the QIAquick PCR Purification Kit according to the manufacturer's instructions (Qiagen). The DNA was eluted in 50 µl of TE buffer and stored at -20°C and its concentration measured by using the Qubit 2.0 Fluorometer (Life Technologies).

3.8. Mitochondrial DNA Extraction

Mitochondrial DNA was isolated using Mitochondrial DNA Isolation Kit (Abcam). Cells (5×10^6) were collected by centrifugation at 600 x g for 5 minutes at 4° C and washed with ice-cold 1X PBS. They were resuspended in 1X cytosol extraction buffer and incubated on ice for 10 minutes. Ice-cold Teflon homogenizer was used to homogenize the cells (50-100 passes) until 70-80 % of nuclei lost their cytoplasmic membranes. The efficiency of homogenization depends on the cell type, therefore the number of passes needed were optimized for HEK293T cells by viewing the homogenized suspension with Trypan blue dye under the EVOS^{TM} XL core microscope (Thermo Fisher Scientific) after different number of passes to avoid excessive homogenization. The homogenate was then centrifuged at 700 x g for 10 minutes at 4°C to remove nuclei and intact cells in the pellet. The cytoplasmic supernatant was centrifuged at 10,000 x g for 30 minutes at 4°C, and the pellet was resuspended in 1X cytosol extraction buffer and centrifuged again. The resulting pellet was isolated mitochondria which was lysed using the mitochondrial lysis buffer. Afterwards, the enzyme mix was added, and the sample was incubated in a 50°C water bath for 60 minutes until the solution became clear. Then, it was centrifuged at maximum speed 17,000 x g for 5 minutes at room temperature following the addition of absolute ethanol at -20°C for 10 minutes. Finally, the mitochondrial DNA pellet was washed with 70 % ethanol and stored in 20 µl

of TE buffer at – 20°C. The quantity of eluted DNA was measured by using the Qubit 2.0 Fluorometer (Life Technologies).

3.9. Western Blot Analysis of Isolated Mitochondrial Fraction

Western blotting of HEK293T subcellular fractions obtained during the mitochondrial DNA isolation protocol (Abcam) was performed using Cell Fractionation Antibody Sampler Kit (Cell Signaling Technology) to check the purity and enrichment of the mitochondrial fraction. Primary antibodies against histone deacetylase 2 (HDAC 2), MAPK or Erk kinases 1/2 (MEK 1/2), and apoptosis-inducing factor (AIF) were used to target proteins that are localized in the nucleus, cytoplasm and mitochondria, respectively. The analyzed samples included total cell lysate, nuclei and intact cells fraction, cytoplasmic fraction, and mitochondrial fraction. The total cell lysate was prepared using HEK293T cells. The cells were washed and harvested from cell culture plates in ice-cold 1X PBS by centrifugation at 300 x g for 3 minutes at 4° C. The cell pellet was resuspended in cold lysis buffer (50 mM Tris-HCl pH 8, 1 mM EDTA, 150 mM NaCl and 0.5% NP-40) containing protease and phosphatase inhibitors and left on ice for 10 minutes. Next, it was sonicated three times (10 seconds each) at a power of 2, with 30-second intervals on ice between sonication cycles, then centrifuged at 4°C and 17,000 x g for 10 minutes. The supernatant was collected in a fresh tube as a total cell lysate and the pellet was discarded. Beside total cell lysate, cellular fractions were collected from HEK293T during successive centrifugation steps previously described in section 3.8 and lysed according to the manufacturer's instructions. The protein concentration of all samples was quantified using the Pierce BCA Protein Assay Kit (Thermo Fisher Scientific) and BSA as a standard, according to the manufacturer's instructions. The protein samples were denatured by 5-minute boiling after the addition of the reducing SDS loading buffer (62.5 mM Tris-HCl pH 6.8, 25% glycerol, 2% SDS, 0.01% bromophenol blue and 5% β-

mercapthoethanol) and then loaded onto a 10% polyacrylamide gel. The SDS polyacrylamide gel electrophoresis (PAGE) was run at 150V for an hour. The proteins were transferred from the polyacrylamide gel to a 0.45 µm nitrocellulose membrane (Bio-Rad) using the Trans-Blot Turbo Transfer System (Bio-Rad) according to the manufacturer's instruction. The membrane was stained with Ponceau S (0.5% Ponceau S and 5% acetic acid) for 5 minutes to check the transfer efficacy and then washed for 5 minutes with ddH_2O. Next, the membrane was baked for 15 minutes at 65°C and blocked with 5% skim milk (5 g skim milk powder in 100 ml of 0.1% TBST (50 mM Tris-HCl pH 7.6, 150 mM NaCl and 0.1% Tween-20)) for an hour on a rocking platform shaker (VWR) at room temperature. After that, the primary antibodies were prepared (1:1000) in 5% skim milk (0.1% TBST) according to the manufacturer's instructions. The membrane was incubated with the selected primary antibody at 4°C overnight on an Orbitron rotator (Boekel Scientific). The following day, the membrane was washed three times with 0.1% TBST (10 minutes each) on the rocking platform shaker at room temperature. Then, a one-hour secondary antibody incubation with the appropriate horseradish peroxidase-conjugated anti-IgG diluted in 5% skim milk was done at room temperature. Following that, the three-washes step with 0.1% TBST was repeated. Finally, the protein bands on the membrane were detected and visualized using Western Lightning Plus-Enhanced Chemiluminescence (ECL) Reagents (Perkin Elmer) on Amersham Hyperfilm ECL (GE Healthcare) according to the manufacturer's instructions.

3.10. Mitochondrial DNA to Nuclear DNA Ratio

Quantitative PCR is an efficient quantitative technique for estimating the relative amount of known DNA in a given sample. Here, qPCR analysis was performed on QuantStudio™ 3 Real-Time PCR System (Thermo Fisher Scientific) using a primer designed for nuclear *GAPDH* and another designed for mitochondrial gene *MTCYB* (**Table 2 and Figure 5**) to measure the mtDNA

to nDNA ratio through calculating the threshold cycle Ct values and comparing the mtDNA copy number relative to the nDNA copy number. Conditions for the qPCR were as follow: (preamplification step) 50°C for 2 minutes and 95°C for 2 minutes, (amplification steps) 40 cycles of 98°C for 15 seconds, 64.5°C for 30 seconds and 72°C for 15 seconds. Lastly, the melting curve steps: 95°C for 15 seconds, 60°C for 1 minute and 95°C for 1 second. The qPCR reactions were prepared to a total volume of 20 µl in each well of 96-well plates on ice. Each reaction was performed in triplicate and composed of 10 ul of the PowerUp SYBR Green Master Mix (Applied Biosystems^{TM}), 0.2 µl of the forward primer (10 µM), 0.2 µl of the reverse primer (10 µM), 1 ng gDNA of $CD4^+$ and $CD8^+$ T cell (set 1,6-10) (for the standard curve using HEK293T cell line: a constant amount (1 ng) of nDNA + dilutions (0, 0.2, 0.4, 0.6, 0.8, 1 ng) of mtDNA) and volumes were brought up to 20 µl with RNase free water (Thermo Fisher Scientific).

Analysis of mtDNA to nDNA ratio was calculated by following the ΔCt method. Ct values were generated using the qPCR machine software and the mean of the triplicate values of Ct for each DNA sample was calculated. The ΔCt calculated using the following formula: ΔCt = Ct (mtDNA gene) −Ct (nDNA gene). Then, the fold change of each sample was measured as $2^{-\Delta Ct}$.

Table 2. List of primers used for determining the mitochondrial to nuclear DNA ratio.

Gene	Primer Sequence	Amplicon size (bp)
MTCYB	**Forward**: 5'- GCG TCC TTG CCC TAT TAC TAT C -3'	**123 bp**
	Reverse: 5'- CTG CGG CTA GGA GTC AAT AAA -3'	
GAPDH	**Forward**: 5'- GTA TGA CAA CGA ATT TGG CTA CAG -3'	**115 bp**
	Reverse: 5'- CTC TCT TCC TCT TGT GCT CTT G -3'	

A.

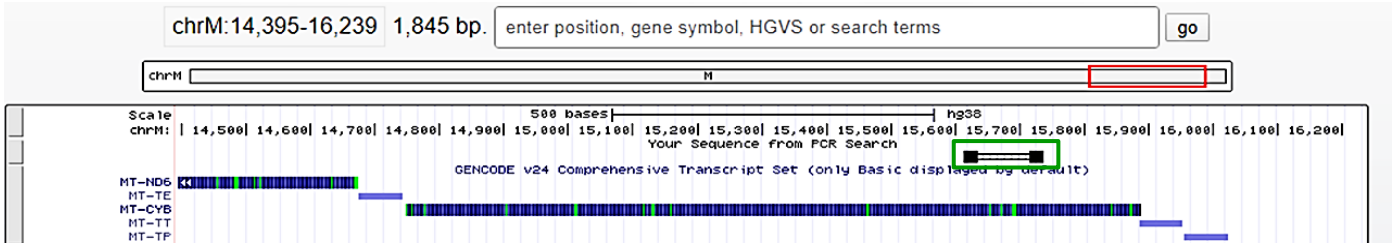

B.

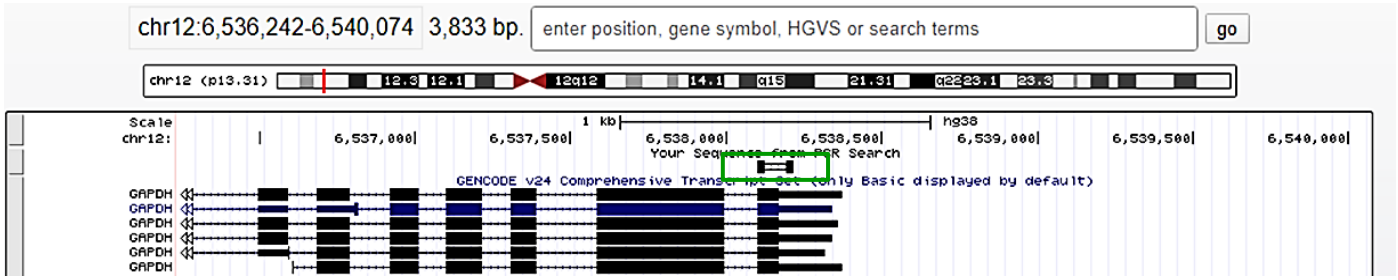

Figure 5. Primer location of *MTCYB* and *GAPDH* used for determining the mitochondrial to nuclear DNA ratio.

Primer location of **A.** mitochondrial *MTCYB* gene and **B.** nuclear *GAPDH* gene. The green box shows the exact location of the amplicon in ENCODE.

CHAPTER FOUR

4.0 RESULTS

4.1. Detection of Mitochondrial DNA Methylation

The presence and patterns of mitochondrial DNA methylation were determined in $CD4^+$ and $CD8^+$ T cells. For this purpose, whole blood samples were collected from 10 healthy individuals and PBMCs were purified by density-gradient centrifugation by Dr. Ruey Su's lab. Then, T cells of interest were isolated by immunomagnetic negative selection to avoid the activation of $CD4^+$ and $CD8^+$ T cells. Following total DNA extraction and sonication (~250 bp), MBD-seq was performed using MethylMiner Methylated DNA Enrichment Kit which is dependent on MBD2 binding to the methylated regions. The MethylMiner kit was first validated for DNA methylation detection using control DNA samples included in the kit: two synthetic (methylated and non-methylated) duplex DNAs and pre-fragmented K-562 DNA. The control capture reaction was followed by endpoint PCR and gel electrophoresis. The results showed that the unbound fraction was only amplified by the non-methylated primer set with no signal detected when methylated primer set was used indicating that all of methylated duplex DNA was captured by MBD beads and leaving only the non-methylated DNA in the supernatant (**Figure 6**).

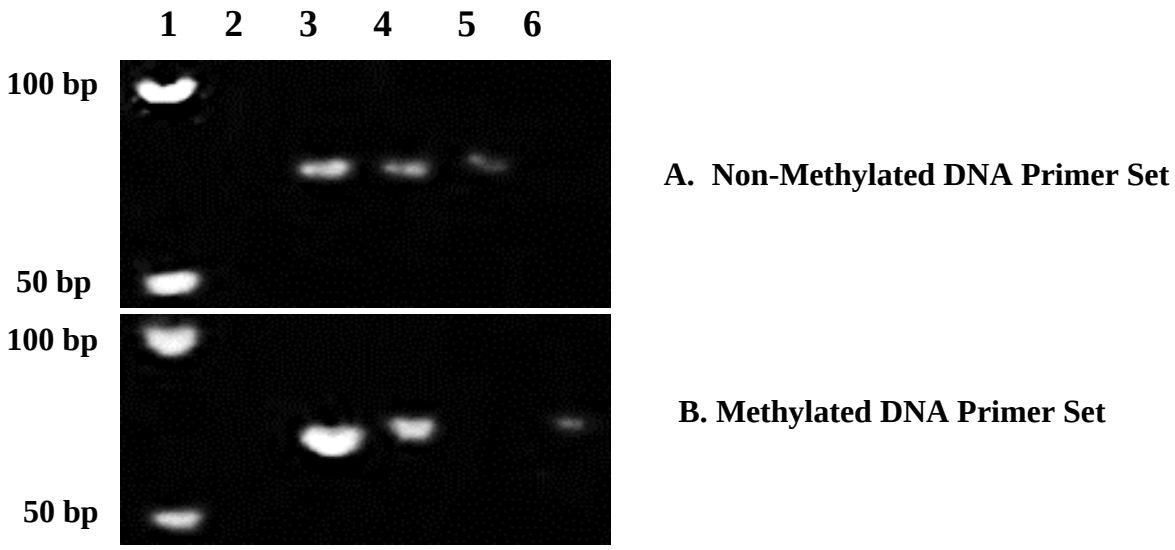

Figure 6. Validation of MethylMiner kit.

Control DNA samples were amplified and loaded onto a 4% agarose gel in parallel with a 50 bp DNA ladder. The size of the control amplicons is 80 bp. The lanes are as follows: 1. 50 bp DNA ladder, 2. Fragmented K-562 DNA, 3. Mix of non-methylated and methylated synthetic DNA, 4. Input DNA (K-562 DNA + mix of non-methylated and methylated synthetic DNA), 5. Unbound (non-methylated) DNA fraction, and 6. Eluted (methylated) DNA fraction. **A.** Bands represent control samples amplified by a primer set specific for non-methylated duplex DNA which include duplex DNA mix, input and unbound DNA. **B.** Bands represent control samples amplified by a primer set specific for methylated duplex DNA which include duplex DNA mix, input and eluted DNA.

Once the MethylMiner kit was validated, isolated DNA from the study samples was sonicated and MBD-coupled magnetic beads were used to enrich for their methylated DNA fragments. The quality check and library preparation for the eluted methylated DNA fragments were completed by Ifeoluwa Adewumi before they were sent to Genome Quebec for sequencing by the Illumina HiSeq 4000 PE 100 sequencer with the depth of 33 million reads per sample. The analysis of MethylMiner sequencing data was done by Dr. Tobias Karakach which involved first the preprocessing of methylation data through PCR duplicate removal and adaptor and quality trimming, then the alignment of reads to the human mitochondrial DNA from Human Genome Assembly GRCh37 (hg19), and the peak calling for methylation by MACS2. The sequencing results of the methylated total DNA fragments isolated from $CD4^+$ and $CD8^+$ T cells confirmed the presence of methylation in the mitochondrial DNA. The distribution of mapped mitochondrial methylation was visualized by the Integrative Genomics Viewer (IGV) revealing variations in the methylation patterns of $CD4^+$ T cells (**Figure 7A**) and $CD8^+$ T cells (**Figure 8A**) across participants. Interestingly, the part of D-loop located at the 3' end of the mitochondrial genome was shown to be methylated in a consistent fashion across these T cells (**Figure 7B, Figure 8B**). Moreover, a number of mitochondrial loci covering genes: *MTND5* for NADH dehydrogenase 5, *MTCO1* for Cytochrome C Oxidase 1 and *MTTS1* for tRNA Serine 1 were found to be significantly methylated in half of the participants (**Table 3**). Also, $CD4^+$ T cells appeared to have a higher number of significantly methylated regions compared to $CD8^+$ T cells in this study group.

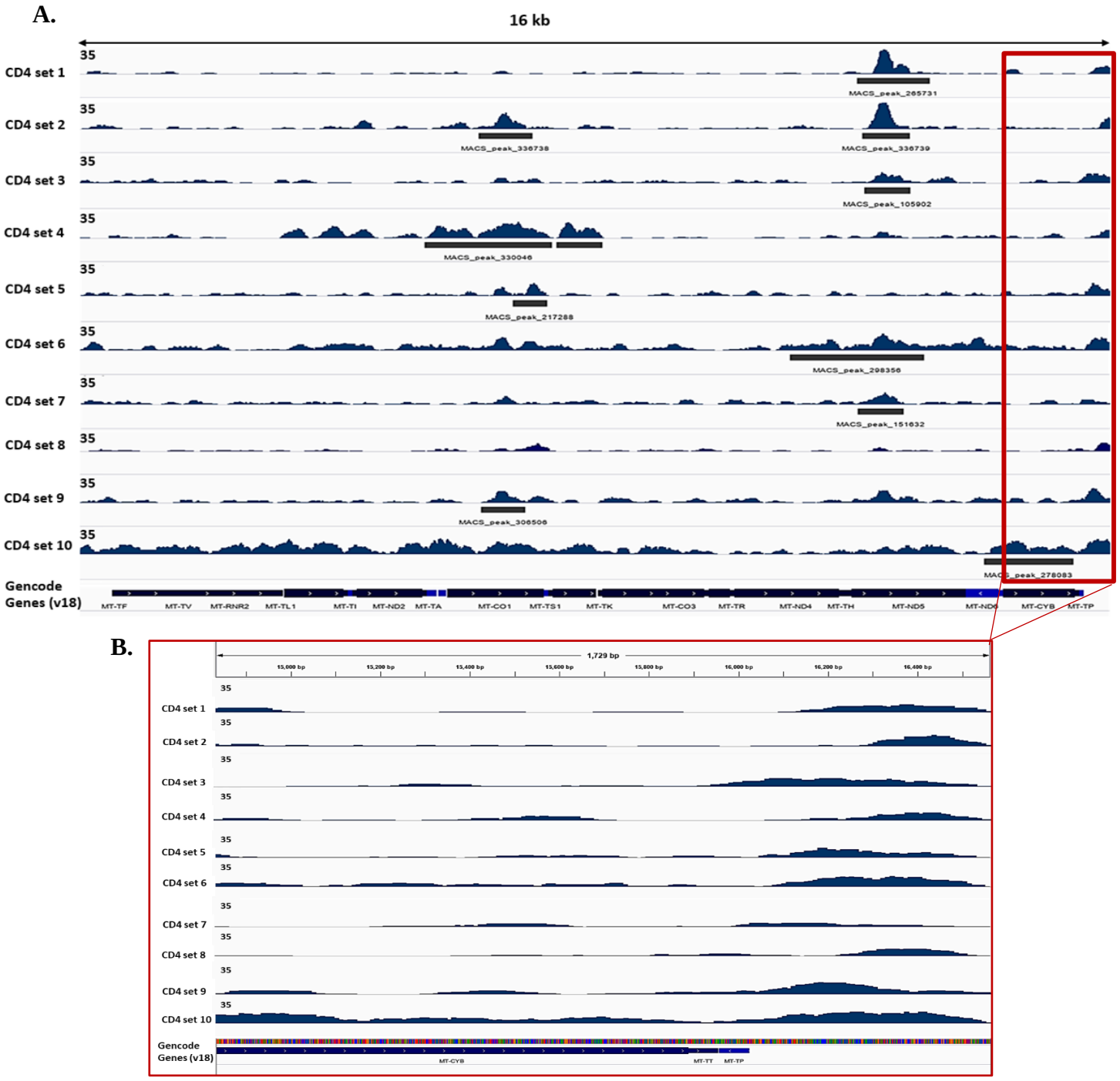

Figure 7. Mitochondrial methylation patterns in CD4⁺ T cells.

A. Variations in mitochondrial methylation patterns were shown across CD4⁺ T cells between study participants (set 1-10). **B.** A zoomed-in (1,729 bp) image of 3'end of mtDNA revealing the overall relative consistency in methylation within the D-loop region. Methylation tracks were generated from MBD-seq and viewed by IGV with the Gencode Genes (v18) reference of mtDNA.

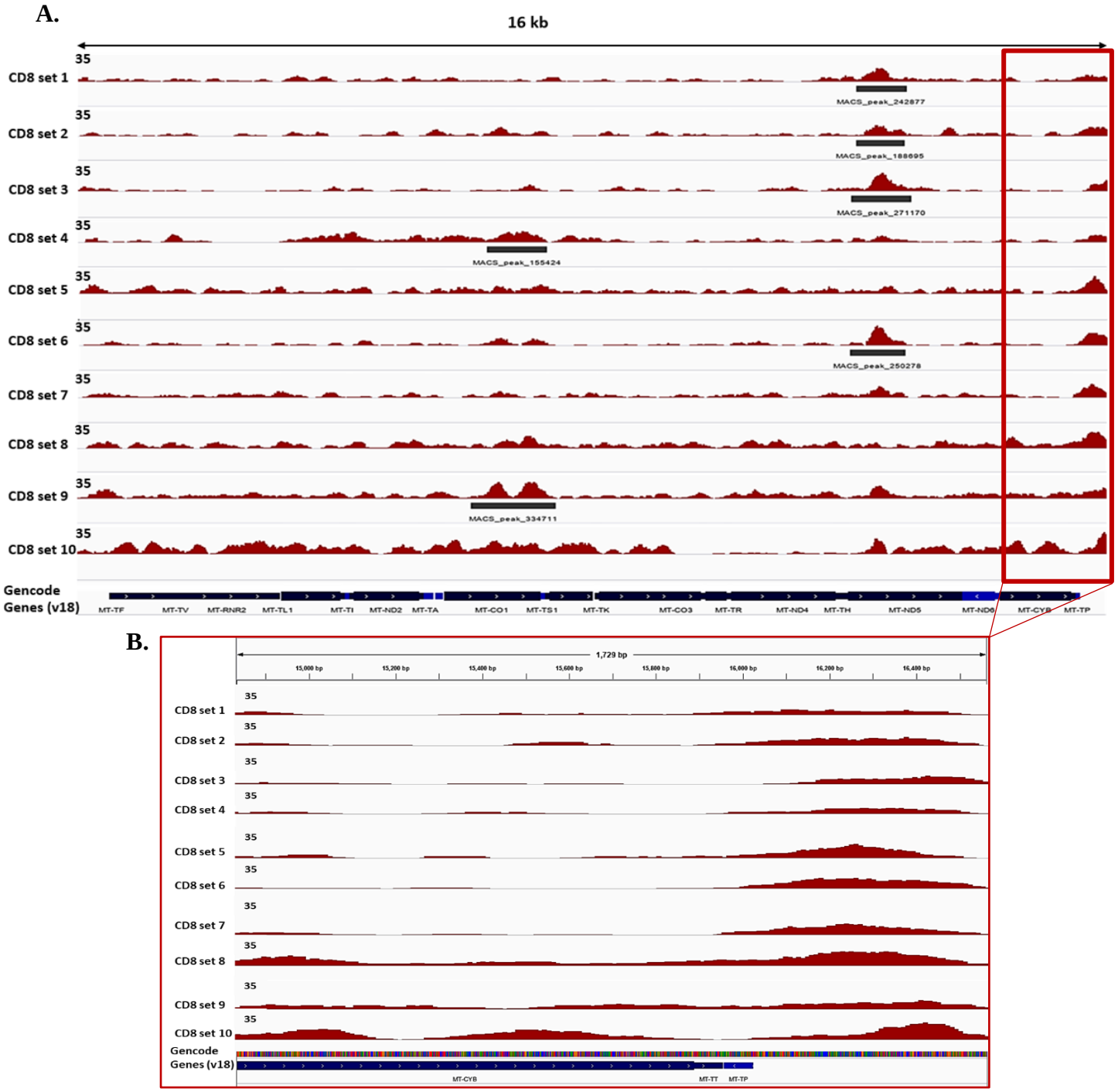

Figure 8. Mitochondrial methylation patterns in CD^{+}8 T cells.

A. Variations in mitochondrial methylation patterns were shown across CD8^{+} T cells between study participants (set 1-10). **B.** A zoomed-in (1,729 bp) image of 3' end of mtDNA revealing the overall relative consistency in methylation within the D-loop region. Methylation tracks were generated from MBD-seq and viewed by IGV with the Gencode Genes (v18) reference of mtDNA.

Table 3. List of mitochondrial genes within the significantly methylated loci of $CD4^+$ and $CD8^+$ T cells across study participants (set 1-10).

Set	T Cell	Genes
Set 1	**CD4**	ND5
	CD8	ND5
Set 2	**CD4**	CO1, ND5
	CD8	ND5
Set 3	**CD4**	ND5
	CD8	ND5
Set 4	**CD4**	TW, TA, TN, TC, TY, CO1, TS1, TD, CO2, TK, ATP8
	CD8	CO1, TS1, TD
Set 5	**CD4**	CO1, TS1
	CD8	---
Set 6	**CD4**	ND4, TH, TS2, TL2, ND5
	CD8	ND5
Set 7	**CD4**	ND5
	CD8	---
Set 8	**CD4**	---
	CD8	---
Set 9	**CD4**	CO1
	CD8	CO1, TS1, TD, CO2
Set 10	**CD4**	ND6, TE, CYB
	CD8	---

4.1. Estimation of DNA Methylation Levels within the Mitochondrial D-loop Region

Following results obtained with the MethylMiner protocol showing consistent methylation pattern within the mitochondrial control region across individuals, bisulfite-pyrosequencing was performed to quantitively estimate methylation of D-loop at single-base resolution. Pyrosequencing is a sequencing-by-synthesis method where regions of interest in the bisulfite-converted DNA are amplified using biotinylated primers and then sequenced. It uses a chemical light reaction to detect the incorporation of deoxynucleotide triphosphates during sequencing and the light signals generated are eventually visualized as peaks. In this study, the primers and assays were designed covering 6 CpG sites positioned at 16328, 16360, 16411, 16427, 16449, 16454 bp respectively within D-loop (**Figure 4**) with the help of Dr. Jones lab. The biotinylated PCR products of bisulfite converted DNA were examined by gel electrophoresis to check the quality of the primer set used. The gel showed successful amplification and no sign of contamination or primer dimer formation (**Figure 9**). The pyrosequencing was done and the percent methylation at each of the targeted CpG sites of interest was calculated by measuring the relative peak height of T versus C at that CpG site. According to the pyrosequencing data generated by the Pyro Q-CpG software, the average methylation level of the six investigated CpG sites in $CD4^+$ and $CD8^+$ T cells was ~ 1% showing a similar pattern in that region of the D-loop in both T cell types across all participants with exception to one outlier (set 10) (**Figure 10**).

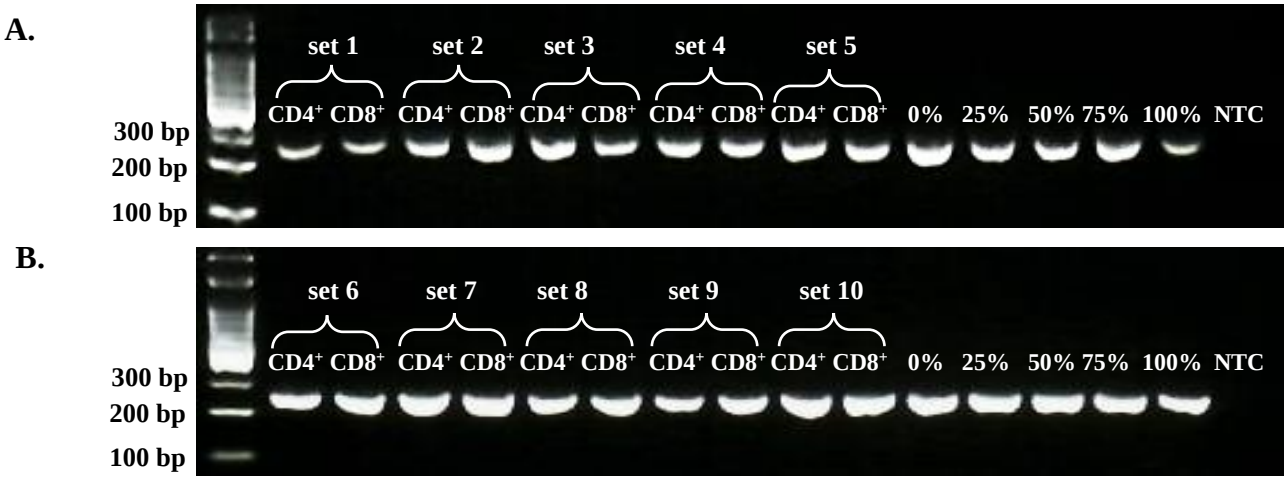

Figure 9. Quality check for PCR amplicons of bisulfite converted DNA samples.

DNA samples were amplified with the forward biotinylated primer and revere primer following bisulfite conversion. The amplicons were loaded onto 1.5% agarose gel in parallel with a 100 bp DNA ladder to test the quality of primer set used. The size of PCR products is 243 bp. **A.** Amplicons from $CD4^+$ and $CD8^+$ T cells (set 1-5) along with 0%, 25%, 50%, 75%, and 100% methylated DNA controls **B.** Amplicons from $CD4^+$ and $CD8^+$ T cells (set 6-10) along with 0%, 25%, 50%, 75%, and 100% methylated DNA controls were examined by agarose gel electrophoresis. A non-template control (NTC) was included both experiments to monitor contamination and primer-dimer formation.

A.

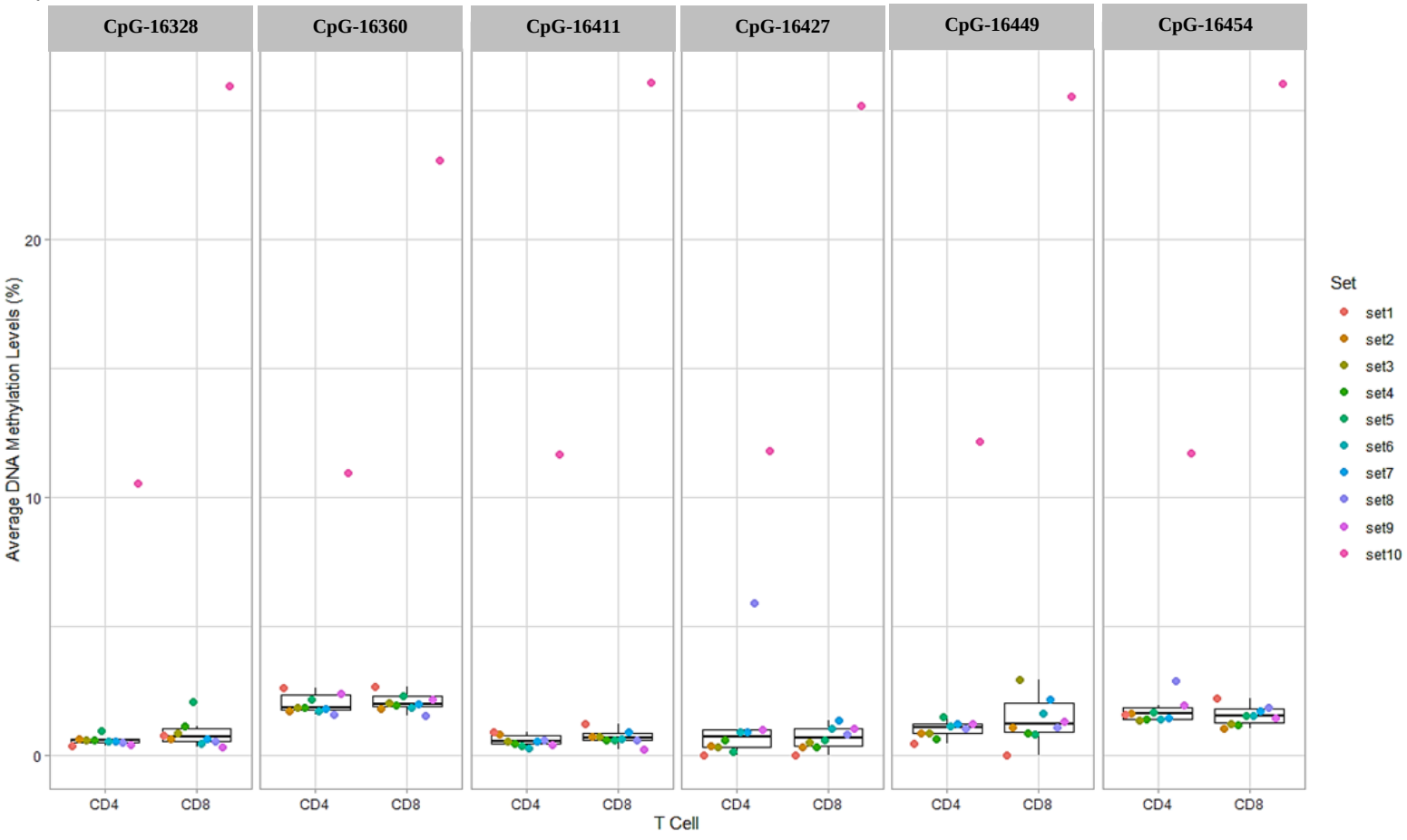
CpG-16328
CpG-16360
CpG-16411
CpG-16427
CpG-16449
CpG-16454
Average DNA Methylation Levels (%)
0
10
20
CD4
CD8
T Cell
Set
set1
set2
set3
set4
set5
set6
set7
set8
set9
set10

B.

Set	T Cell	Methylation Levels (%)						
		D-Loop						
		CpG_16328	CpG_16360	CpG_16411	CpG_16427	CpG_16449	CpG_16454	Average all sites
Set 1	**CD4**	0.3	2.6	0.9	0.0	0.5	1.6	**1.0**
	CD8	0.8	2.7	1.2	0.0	0.0	2.2	**1.2**
Set 2	**CD4**	0.6	1.7	0.8	0.4	0.9	1.6	**1.0**
	CD8	0.6	1.8	0.7	0.3	1.1	1.0	**0.9**
Set 3	**CD4**	0.6	1.8	0.6	0.3	0.8	1.4	**0.9**
	CD8	0.9	2.0	0.7	0.5	2.9	1.2	**1.4**
Set 4	**CD4**	0.6	1.8	0.4	0.6	0.6	1.4	**0.9**
	CD8	1.1	1.9	0.6	0.3	0.9	1.2	**1.0**
Set 5	**CD4**	0.9	2.2	0.4	0.2	1.5	1.7	**1.2**
	CD8	2.1	2.3	0.6	0.6	0.8	1.5	**1.3**
Set 6	**CD4**	0.5	1.7	0.3	0.9	1.1	1.4	**1.0**
	CD8	0.5	1.9	0.6	1.0	1.6	1.6	**1.2**
Set 7	**CD4**	0.6	1.8	0.6	0.9	1.2	1.4	**1.1**
	CD8	0.7	2.0	0.9	1.4	2.2	1.7	**1.5**
Set 8	**CD4**	0.5	1.6	0.6	5.9	1.0	2.9	**2.1**
	CD8	0.5	1.5	0.6	0.8	1.1	1.9	**1.1**
Set 9	**CD4**	0.4	2.4	0.4	1.0	1.2	1.9	**1.2**
	CD8	0.3	2.2	0.2	1.1	1.3	1.4	**1.1**
Set 10	**CD4**	10.6	11.0	11.7	11.8	12.2	11.7	**11.5**
	CD8	26.0	23.1	26.1	25.2	25.5	26.1	**25.3**

Figure 10. Pyrosequencing results of $CD4^+$ and $CD8^+$ T cells.

A. Average methylation levels of 6 CpG sites positioned at 16328, 16360, 16411, 16427, 16449 and 16454 bp within the mitochondrial D-loop of $CD4^+$ and $CD8^+$ T cells from the study participants (set 1-10). Boxplots graph generated using R software. All samples were run in triplicates. **B.** Table summarizing the average methylation percentages of T cells at all 6 sites.

4.2. Mitochondrial DNA Content in $CD4^+$ and $CD8^+$ T Cells

The purpose of estimating the mitochondrial to nuclear DNA ratio was to get an idea of the relative amount of mitochondrial DNA which could influence the methylation level in a cell type. Prior to running the qPCR for mitochondrial to nuclear DNA ratio, mitochondrial DNA isolation protocol was optimized. The Abcam protocol instructed homogenizing cells with 50-100 strokes depending on cell type until 70-80% of nuclei lose their cell membrane. HEK293T cells were used for their rapid reliable growth and their homogenization was optimized for. The homogenized suspension was viewed under the microscope at different points after 50, 70 and 90 strokes and their resulting mtDNA yield was compared (**Figure 11**). The optimal number of strokes was determined to be 70 as it resulted in the highest mtDNA yield without excessive loss and damage of mitochondria.

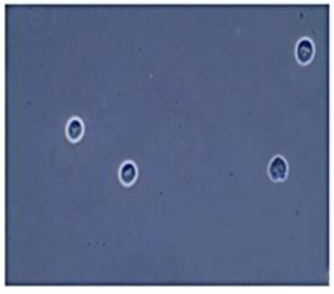	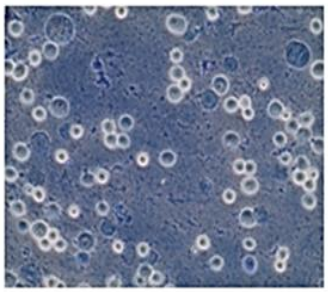	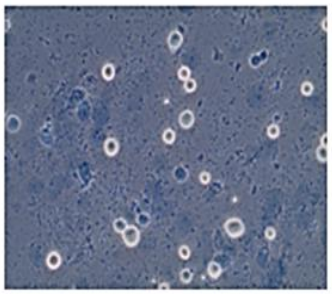	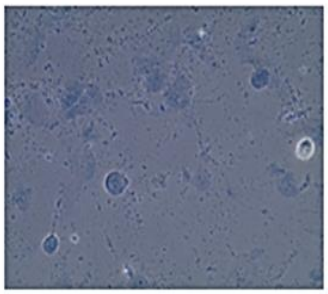
0 strokes	**50 strokes**	**70 strokes**	**90 strokes**
mtDNA yield	**52.6 ng/µl**	**74.2 ng/µl**	**57.4 ng/µl**

Figure 11. Optimization of mitochondrial DNA isolation protocol.

HEK 293T (~ 5 x 10^6) cells were collected and resuspended in cytosol extraction buffer. Microscopic images (X10 with Trypan blue dye) were taken of cells (from left to right) before homogenization, and after 50, 70 and 90 strokes with Teflon homogenizer. The shiny ring around the nuclei indicate intact cell membrane, thus with 70 strokes, 70-80 % of nuclei appeared to lose the shiny ring while with 50 and 90 strokes, they either mainly intact or lose it all. The mtDNA yield was measured with the Qubit 2.0 Fluorometer (Life Technologies) and higher amount of mtDNA was obtained with 70 strokes.

Nuclear DNA was isolated using a nuclear isolation protocol which involved cell lysis using cell lysis buffer and a syringe, then further with SDS as well as treatment with RNase and Protease enzymes. Mitochondrial DNA was isolated using Mitochondrial DNA Isolation protocol (Abcam) through homogenization with cytosol extraction buffer followed by a series of centrifugation steps. The mitochondria were then lysed and mtDNA was purified with the addition of enzyme mix and ethanol. Western blot analysis of cellular fractions obtained during the mitochondrial DNA isolation protocol was performed to check the mitochondrial fraction. It showed an effective enrichment of the mitochondrial fraction; however, the weak signal detected by HDAC2 and MEK1/2 antibodies indicate a mild contamination of the mitochondrial pellet with nuclear and cytoplasmic supernatant during isolation (**Figure 12**). Finally, qPCR was performed to measure the mitochondrial to nuclear DNA ratio using a nuclear *GAPDH* and mitochondrial *MTCYB* primers and gDNA of $CD4^+$ and $CD8^+$ T cells (set 1,6-10). The resulting linear standard curve (**Figure 13A**) was run using a constant amount (1ng) of nDNA and dilutions (0, 0.2, 0.4, 0.6, 0.8, 1 ng) of mtDNA. The mitochondrial to nuclear DNA ratio analysis showed variability between $CD4^+$ and $CD8^+$ T cells across individuals reflecting disparity in their relative endogenous mitochondrial DNA content even within the same cell type (**Figure 13B**).

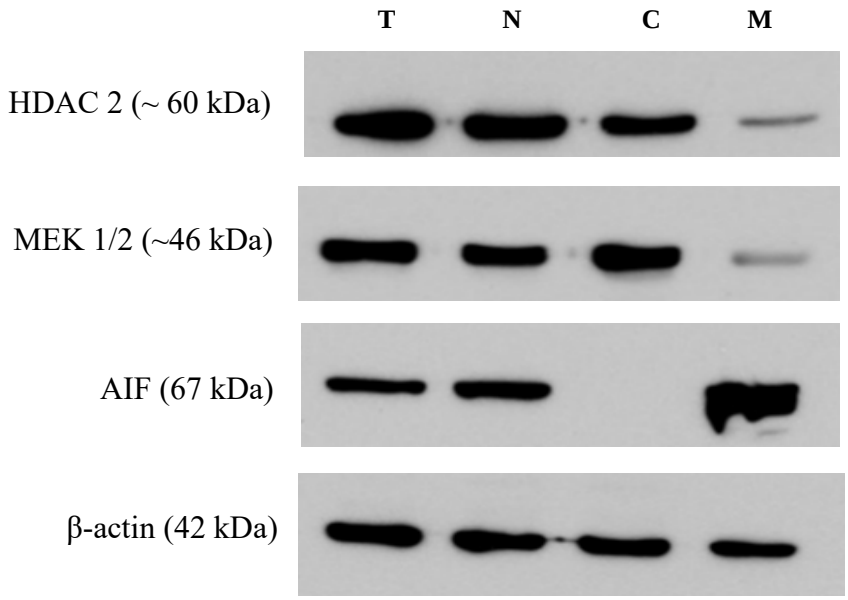

Figure 12. Verification of mitochondrial fraction enrichment.

Western blot analysis was done for subcellular fractions obtained during the mitochondrial DNA isolation protocol (Abcam) to check the purity and enrichment for the mitochondrial fraction. The HEK293T cell line was used. Fraction samples were as follows: total cell lysate (T), nuclei and intact cells fraction (N+IC), cytoplasmic fraction (C), and mitochondrial fraction (M). The use primary antibodies were against histone deacetylase 2 (HDAC 2), MAPK or Erk kinases (MEK 1/2), and apoptosis-inducing factor (AIF) which serve as markers for the nucleus, cytoplasm, and mitochondria, respectively. β-actin was used as a loading control for western blot.

A.

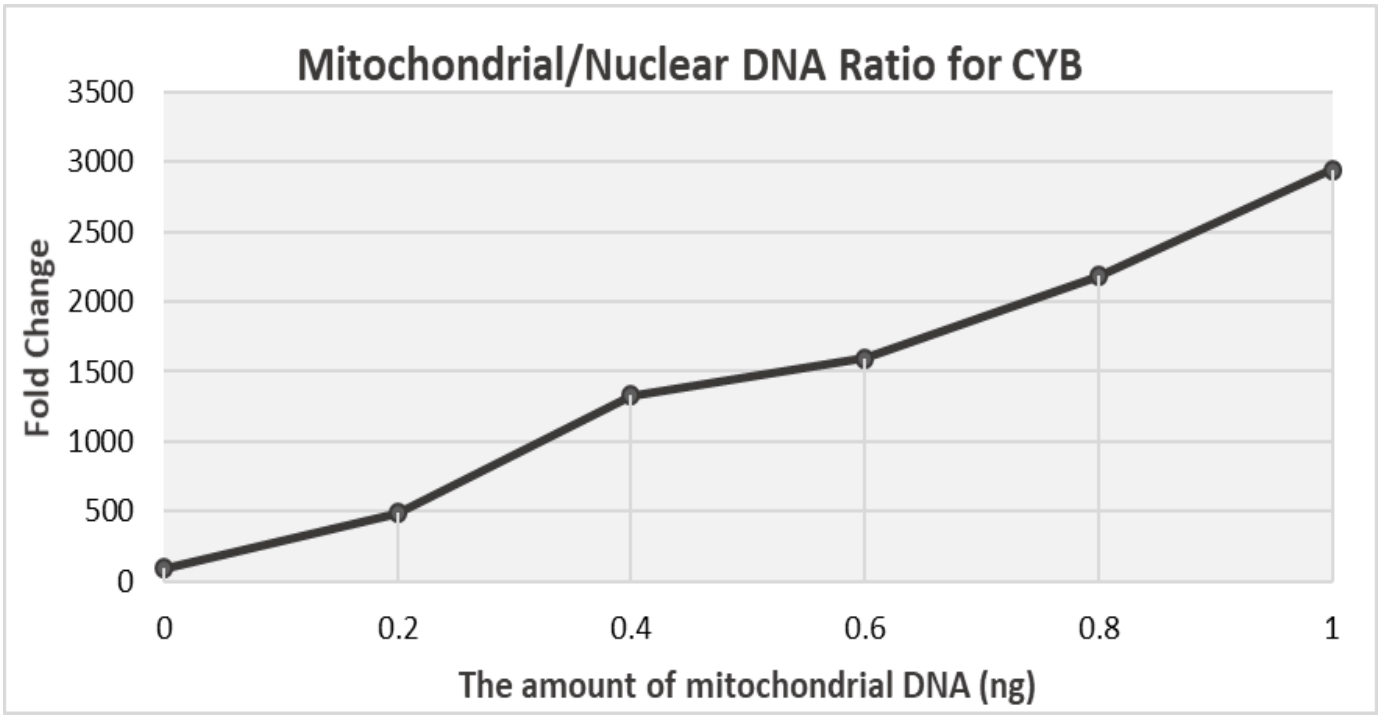

B.

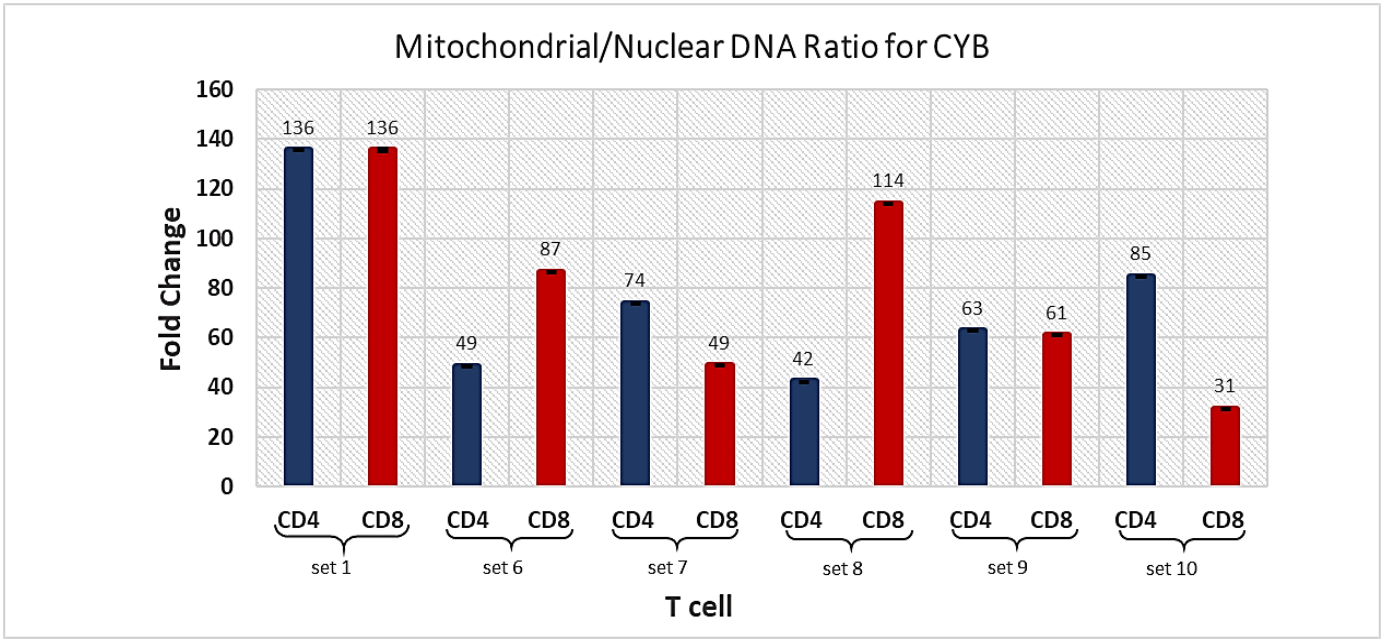

Figure 13. Mitochondrial to nuclear DNA ratio results.

A. Quantitative PCR resulted in a linear standard curve for *MTCYB* with increasing amount of mtDNA. **B.** Mitochondrial to nuclear DNA ratio results for $CD4^+$ and $CD8^+$ T cells of sets 1, 6, 7, 8, 9, and 10 was calculated using ΔCt method and plotted in a bar graph. All samples were run in triplicates. Error bars represent standard error of mean.

CHAPTER FIVE

5.0 DISCUSSION

5.1. Human Mitochondrial DNA Methylation in $CD4^+$ and $CD8^+$ T cells

The present study, to the best of our knowledge, is the first to use MBD-seq to study mitochondrial genome wide coverage of 5-mC. Although MBD-seq provides ~150 bp resolution rather than single base pair resolution, MBD proteins are very specific to methylated cytosines and do not interact with hydroxymethylated cytosines. In addition, this method requires relatively less time and money compared to other techniques (Aberg, Chan, Xie, Shabalin, & van den Oord, 2018). To establish baseline methylation patterns within the mitochondrial genome, normal $CD4^+$ and $CD8^+$ T cells derived from human blood were assessed. Immunomagnetic negative selection method was used to isolate these cells to avoid any possible activation and maintain their function unaltered. In line with previous observations from literature (Pirola et al., 2013; Shock et al., 2011), this methodology proved that human mitochondrial genome is indeed methylated. Considering the different variations in mitochondrial methylome patterns observed in $CD4^+$ and $CD8^+$ T cells across different individuals, these results demonstrated the generality and cell-type specificity of baseline mtDNA methylation. Interestingly, the findings also revealed that the 3' end in the terminal part of D-loop region displayed consistency in its methylation across all samples. Moreover, a few significantly methylated regions were identified in $CD4^+$ and $CD8^+$ T cells. In half of the participants, these regions were found to harbor *MTND5, MTCO1* and *MTTS1* which encode for NADH dehydrogenase 5, Cytochrome C Oxidase 1 (both involved in oxidative phosphorylation), and TRNA Serine 1 (involved in mtDNA translation), respectively. Subsequently, bisulfite pyrosequencing was conducted to quantitatively further estimate the methylation degree of 6 CpG sites positioned at 16328, 16360, 16411, 16427, 16449, 16454 bp

respectively within that part of D-loop region. The average methylation value of the six CpG sites in the D-loop across all participants, with exception to set 10 (11.5% for $CD4^+$ and 25.3% for $CD8^+$) was estimated to be ~1%. However, the possibility that other CpG sites that were not analyzed might be methylated at higher level cannot be excluded. Further investigation with other methods may help confirm those findings and eliminate any possible bias in methodologies used for this study.

The accuracy of mtDNA methylation depends primarily on the methodology used. The existing methylation analysis techniques have been designed with the purpose of investigating the nuclear DNA. Given the structural and functional differences between nDNA and mtDNA, modification of these techniques is needed. There are some aspects to the methodologies used in this study specific for mtDNA. Total gDNA (nDNA+ mtDNA) was isolated from cells instead of just mtDNA followed by the extraction of mitochondrial genome reads during the bioinformatic analysis step. Although, Liu et al. (2016) reported that the circular structure of mtDNA reduces the bisulfite conversion efficiency, leading to overestimation of mtDNA methylation values, no linearization of the mtDNA was done prior to bisulfite conversion for this analysis with pyrosequencing. The previously mentioned study listed the failed inner quality control due to incomplete bisulfite conversion, the signal loss due to insufficient PCR product and uncertain reference sequence pattern as main reasons for the lower success rate of bisulfite pyrosequencing using the circular mtDNA when compared to the BamHI-linearized mtDNA (Liu et al., 2016). During bisulfite treatment, all unmodified cytosines are converted to uracil while the modified cytosines remain unchanged, then the methylation can be quantified by calculating the C to T ratio. In case of incomplete bisulfite conversion, the ratio will be increased due to unmodified cytosines left unconverted, thus counted as cytosine. Surprisingly, none of the issues discussed by the paper

(Liu et al., 2016) were encountered in this study as the sample group had passed the inner quality control, adequate PCR product was achieved, and no signal loss was reported. Despite the difference in approach, the present study showed very low methylation levels (~1%) in D-loop of $CD4^+$ and $CD8^+$ T cells similar to the methylation value (1.16 %) reported for linearized mtDNA D-loop in human blood. One possible explanation is that the harsh conditions that the DNA is subjected to during bisulfite treatment resulting in the fragmentation and degradation of treated DNA, might have possibly led mtDNA to lose its circular structure. It should also be noted that the inability of bisulfite conversion-based methods to differentiate between 5-mC and 5-hmC could possibly impact the methylation levels, however it is yet to be determined the extent to which this fact contribute to the overestimation of methylation values and whether it should considered a reliable method for future studies.

Further complications could be potentially raised when analyzing mtDNA methylation given the triple-stranded nature of the D-loop which could affect the reliability of bisulfite pyrosequencing results. The D-loop is formed by the incorporation of a linear third DNA strand 7S DNA of approximately 650 bp which originates from a premature termination of H-strand replication (Nicholls & Minczuk, 2014). However, the factors controlling D-loop synthesis and turnover are hardly known. Previous reports have indicated the possibility of 7S DNA amplification instead of H-strand as a third strand of template by primers designed to target the D-loop depending on the fraction of mtDNA used for the study (B. Li et al., 2018). This would be misleading in cases such as mitochondrial copy number studies resulting in as a false positive. However, the effect of 7S DNA amplification on the D-loop methylation levels estimated by bisulfite pyrosequencing remains to be investigated.

A recent study revealing higher mitochondrial methylation in a non-CpG (CpA, CpT, CpC) context than that of CpG (Patil et al., 2019) might provide an explanation to the lower methylation level when detected by the CpG dinucleotide-biased methylation techniques. The observed non-CpG methylation was reported to follow a predominantly conserved pattern of methylation in cell types where 5-mCpC > 5-mCpA / 5-mCpT > 5-mCpG; however, the functional significance of this consistency remains unknown. The study further showed a potential link between methylation in the L strand promoter and a reduction of *MTND6* expression in different cell types, suggesting a strand-specific regulatory role of methylation in gene expression. Moreover, Van Der Wijst et al. (2017) proposed that mtDNA methylation in the GpC context rather than CpG within the promoter region might be the one influencing the mitochondrial gene expression. However, it should be noted that an exogenous methyltransferase was used in the study to induce methylation and its biological validity is in question. An interesting discovery was made by Koh et al. (2018) where another form of methylation at the adenine base as found to be enriched (>8000x) in mtDNA than in nDNA using 6-mA-crosslink-exonuclease sequencing. The proposed functional role of 6-mA was linked to mtDNA replication through mediating the melting of double stranded mtDNA and recruitment of mtSSB. Taking into account the endosymbiotic origin of mitochondria, this holds out the possibility that, unlike the nDNA, mtDNA methylation might be predominantly on the adenine leading the way to another exciting area for future investigation.

Another key point to mention is that the homology between mitochondrial DNA and NUMTs may cause misleading results when analyzing mitochondrial sequencing data. In case of next generation sequencing data analysis, mtDNA and NUMTs reads cross-alignment can occur, resulting in the detection of false positive reads where NUMTs short reads aligning to chromosome M or false negatives where mtDNA reads are lost for their alignment to NUMTs

sequences (Maude et al., 2019). However, it is still highly unlikely for NUMTs to significantly contribute to methylation or get amplified in the first place due to the excessive amount of mtDNA (1000-10,000 copies per cell) compared to nDNA (2 copies per cell) (Lightowlers, Chinnery, Turnbull, Howell, & Turnbuu, 1997). Moreover, data from this study were uniquely mapped to the human mitochondrial DNA from Human Genome Assembly GRCh37 (hg19) and NUMTs were filtered.

Finally, this study is limited by the unavailability of sufficient sample size to precisely estimate the extent of methylation and identify significant relationships between the data. Furthermore, the study design could have been enhanced by establishing stricter inclusion criteria when selecting participants to ensure reaching to a more solid and informative conclusion which can be generalized to a larger population. Another limitation is the inability to compare the methylation patterns obtained in this study using total gDNA with that generated from exclusively purified mitochondrial DNA to confirm and test the reliability of results due to the fact that a sufficiently large number of $CD4^+$ and $CD8^+$ T cells from blood samples was not available for mitochondrial DNA extraction.

5.2. The Effect of Mitochondrial DNA Content in $CD4^+$ and $CD8^+$ T cells on Methylation

In this study, the link between mtDNA methylation and mtDNA content in $CD4^+$ and $CD8^+$ T cells was also investigated. There are multiple copies of mtDNA in each cell depending on their cellular energy requirement. Cells with high demand for oxidative phosphorylation-generated ATP have higher copy number than those with lower demand. The mtDNA content is strictly regulated by specific nuclear-encoded replication factors with the key factor being POLγ which is in turn regulated by DNA methylation (Kelly, Mahmud, McKenzie, Trounce, & St John, 2012). Notably, research has suggested that mtDNA gene expression may be indirectly (Williams, 1986)

influenced by its methylation through regulation of mtDNA replication (Bellizzi et al., 2013; Bianchessi et al., 2016). Alternatively, mtDNA copy number was shown to be able to modulate the methylation of nDNA genes, some of them involved in regulation of oxidative stress-induced apoptosis (Smiraglia, Kulawiec, Bistulfi, Gupta, & Singh, 2008). Hence, mtDNA methylation might be recognized as an important player in the nuclear-mitochondrial crosstalk to maintain cellular functions. Nevertheless, the possible effect of mtDNA copy number on mtDNA methylation requires further investigation and remains largely unexplored. Our findings showed no evidence supporting any potential effect of mtDNA cellular content on mtDNA methylation patterns. The inconsistency in the relative mitochondrial content of $CD4^+$ and $CD8^+$ T cells across individuals (set 1,6-10) made it difficult to identify any sort of pattern when compared to their methylation distribution. Moreover, the pyrosequencing data made it unlikely for the equally low methylation levels observed across individuals to be influenced by their mtDNA content.

5.3. Conclusion and Significance

In summary, this study is the first to analyze the cytosine methylation in the human mitochondrial genome of $CD4^+$ and $CD8^+$ T cells from healthy individuals using MBD-seq. The mitochondrial DNA is in fact methylated and the level of methylation is very low. The pattern and distribution of methyl cytosines are relatively variable in the different cells and individuals, with the exception of the 3' end in the terminal part of D-loop which appear to be constant to a certain extent across the mitochondrial genome with the average methylation level of ~ 1%. Additionally, no association observed between the mtDNA methylation distribution in $CD4^+$ and $CD8^+$ T cells and their relative mtDNA content.

The observed variability in methylation of cells might potentially influence variable genetic regulation and associated phenotypic variation. Also, the mitochondrial primary function of

maintaining the cellular energy demand has made it highly responsive to external conditions, thus methylation can be a potential mechanism used by the mitochondria to transiently regulate gene expression and modulate its responses. Since the functional importance of D-loop as a control region containing promoters and origin of replication, its methylation may have regulatory consequences on mitochondrial replication and transcription in a cell-specific manner. However, the detected low level of methylation by this study in that region deems it unlikely that methylation will have any major impact on mitochondrial function and maintenance. Similarly, given the amount of variations on both inter- and intra-individual level, mitochondrial DNA methylation does not have the required criteria to be used as a standard "diagnostic" biomarker. Additionally, studies have characterized the influence of sex and age on methylation patterns in nuclear genome (Unnikrishnan et al., 2019). As such, it should be noted that both sex and age could possibly impact mtDNA methylation and have also influenced the results found in this study. Nevertheless, it might be more informative if the mitochondrial methylation was studied on an individual basis for a particular cell type prior and after their disease development, environmental exposure or drug treatment. Therefore, further comprehensive experimental studies aimed at proving the biological significance of mtDNA methylation and its potential clinical applications are required for normal physiological and pathological states.

5.4. Future Directions

To further investigate the mtDNA methylation of $CD4^+$ and $CD8^+$ T cells, several experiments are proposed, and a larger sample size of healthy participants will need to be recruited. A sufficient number of T cells will be collected to be able to exclusively isolate mitochondrial genome which in turn makes the process of filtering mtDNA sequencing data easier than that of total gDNA. Moreover, expanding the quantitative estimation of methylation using bisulfite-

pyrosequencing to cover the entire D-loop, especially the promoter regions HSP and LSP as well as origin of replication O_H will be done to identify any significant levels of 5-mC there. Also, it is important to keep in mind the differences between the mtDNA and nDNA and to look at mtDNA methylation from a new angle. Thus, the CpC, CpA and CpT methylation as well as adenine methylation will be investigated. Adenine methylation will be measured using 6-mA-crosslink-exonuclease sequencing which provides a genome-wide mapping of 6-mA with single nucleotide resolution. MBD-seq is not suitable to study the non-CpG methylation since it only captures 5-mC at CpG dinucleotides. Given the fact that bisulfite-based sequencing does not distinguish between 5-mC and 5-hmC, investigators (Booth et al., 2012) have altered the bisulfite chemistry to get around this problem and produced oxBS-Seq. The oxBS-Seq uses potassium perruthenate to oxidize 5-hmC to 5-fC while leaving unmodified cytosine and 5-mC unchanged. The differences between 5-hmC and 5-mC is demonstrated when bisulfite converts 5-fC and unmodified cytosine to uracil leaving 5-mC untouched.

Another exciting experiment to consider is the purification of $CD4^+$ and $CD8^+$ T cells and culturing them *in vitro* laboratory conditions. Then, they will be used to examine the methylation machinery components including the methyl donor and methyltransferases and their translocation to the mitochondria via western blotting and confocal fluorescent microscopy. Once the enzymes are detected, their effect on methylation will be tested by knocking them down using small interfering RNAs.

REFERENCES

Aberg, K. A., Chan, R. F., Xie, L., Shabalin, A. A., & van den Oord, E. J. C. G. (2018). Methyl-CpG-binding domain sequencing: MBD-seq. In *Methods in Molecular Biology* (Vol. 1708, pp. 171–189). https://doi.org/10.1007/978-1-4939-7481-8_10

Agaronyan, K., Morozov, Y. I., Anikin, M., & Temiakov, D. (2015). Replication-transcription switch in human mitochondria. *Science*, *347*(6221), 548–551. https://doi.org/10.1126/science.aaa0986

Amunts, A., Brown, A., Toots, J., Scheres, S. H. W., & Ramakrishnan, V. (2015). The structure of the human mitochondrial ribosome. *Science*, *348*(6230), 95–98. https://doi.org/10.1126/science.aaa1193

Anderson, O. S., Sant, K. E., & Dolinoy, D. C. (2012, August). Nutrition and epigenetics: An interplay of dietary methyl donors, one-carbon metabolism and DNA methylation. *Journal of Nutritional Biochemistry*, Vol. 23, pp. 853–859. https://doi.org/10.1016/j.jnutbio.2012.03.003

Anderson, S., Bankier, A. T., Barrell, B. G., De Bruijn, M. H. L., Coulson, A. R., Drouin, J., … Young, I. G. (1981). Sequence and organization of the human mitochondrial genome. *Nature*, *290*(5806), 457–465. https://doi.org/10.1038/290457a0

Armstrong, D. A., Green, B. B., Blair, B. A., Guerin, D. J., Litzky, J. F., Chavan, N. R., … Marsit, C. J. (2016). Maternal smoking during pregnancy is associated with mitochondrial DNA methylation. *Environmental Epigenetics*, *2*(3), dvw020. https://doi.org/10.1093/eep/dvw020

Barros-Silva, D., Marques, C. J., Henrique, R., & Jerónimo, C. (2018, September 1). Profiling DNA methylation based on next-generation sequencing approaches: New insights and

clinical applications. *Genes*, Vol. 9. https://doi.org/10.3390/genes9090429

Baughman, J. M., Perocchi, F., Girgis, H. S., Plovanich, M., Belcher-Timme, C. A., Sancak, Y., … Mootha, V. K. (2011). Integrative genomics identifies MCU as an essential component of the mitochondrial calcium uniporter. *Nature*, *476*(7360), 341–345. https://doi.org/10.1038/nature10234

Bellizzi, D., D'aquila, P., Scafone, T., Giordano, M., Riso, V., Riccio, A., & Passarino, G. (2013). The control region of mitochondrial DNA shows an unusual CpG and non-CpG methylation pattern. *DNA Research*, *20*(6), 537–547. https://doi.org/10.1093/dnares/dst029

Berk, A. J., & Clayton, D. A. (1974). Mechanism of mitochondrial DNA replication in mouse L-cells: Asynchronous replication of strands, segregation of circular daughter molecules, aspects of topology and turnover of an initiation sequence. *Journal of Molecular Biology*, *86*(4), 801–824. https://doi.org/10.1016/0022-2836(74)90355-6

Bianchessi, V., Vinci, M. C., Nigro, P., Rizzi, V., Farina, F., Capogrossi, M. C., … Lauri, A. (2016). Methylation profiling by bisulfite sequencing analysis of the mtDNA Non-Coding Region in replicative and senescent Endothelial Cells. *Mitochondrion*, *27*, 40–47. https://doi.org/10.1016/j.mito.2016.02.004

Bochtler, M., Kolano, A., & Xu, G. L. (2017). DNA demethylation pathways: Additional players and regulators. *BioEssays*, *39*(1), 1–13. https://doi.org/10.1002/bies.201600178

Bogenhagen, D. F. (2012, September). Mitochondrial DNA nucleoid structure. *Biochimica et Biophysica Acta - Gene Regulatory Mechanisms*, Vol. 1819, pp. 914–920. https://doi.org/10.1016/j.bbagrm.2011.11.005

Bogenhagen, D. F., Wang, Y., Shen, E. L., & Kobayashi, R. (2003). Protein components of mitochondrial DNA nucleoids in higher eukaryotes. *Molecular & Cellular Proteomics :*

MCP, *2*(11), 1205–1216. https://doi.org/10.1074/mcp.M300035-MCP200

Booth, M. J., Branco, M. R., Ficz, G., Oxley, D., Krueger, F., Reik, W., & Balasubramanian, S. (2012). Quantitative sequencing of 5-methylcytosine and 5-hydroxymethylcytosine at single-base resolution. *Science*, *336*(6083), 934–937. https://doi.org/10.1126/science.1220671

Borowski, L. S., Dziembowski, A., Hejnowicz, M. S., Stepien, P. P., & Szczesny, R. J. (2013). Human mitochondrial RNA decay mediated by PNPase-hSuv3 complex takes place in distinct foci. *Nucleic Acids Research*, *41*(2), 1223–1240. https://doi.org/10.1093/nar/gks1130

Byun, H.-M., Panni, T., Motta, V., Hou, L., Nordio, F., Apostoli, P., … Baccarelli, A. A. (2013). Effects of airborne pollutants on mitochondrial DNA Methylation. *Particle and Fibre Toxicology*, *10*(1), 18. https://doi.org/10.1186/1743-8977-10-18

Byun, H. M., & Barrow, T. M. (2015). Analysis of pollutant-induced changes in mitochondrial DNA methylation. In *Mitochondrial Medicine* (Vol. 2, pp. 271–283). https://doi.org/10.1007/978-1-4939-2288-8_19

Cadenas, E., & Davies, K. J. A. (2000). Mitochondrial free radical generation, oxidative stress, and aging. *Free Radical Biology and Medicine*, *29*(3–4), 222–230. https://doi.org/10.1016/S0891-5849(00)00317-8

Cerritelli, S. M., Frolova, E. G., Feng, C., Grinberg, A., Love, P. E., & Crouch, R. J. (2003). Failure to produce mitochondrial DNA results in embryonic lethality in Rnaseh1 null mice. *Molecular Cell*, *11*(3), 807–815. https://doi.org/10.1016/S1097-2765(03)00088-1

Chan, D. C. (2012). Fusion and Fission: Interlinked Processes Critical for Mitochondrial Health. *Annual Review of Genetics*, *46*(1), 265–287. https://doi.org/10.1146/annurev-genet-110410-

132529

Chang, C. R., & Blackstone, C. (2010). Dynamic regulation of mitochondrial fission through modification of the dynamin-related protein Drp1. *Annals of the New York Academy of Sciences*, *1201*, 34–39. https://doi.org/10.1111/j.1749-6632.2010.05629.x

Chang, D. D., & Clayton, D. A. (1985). Priming of human mitochondrial DNA replication occurs at the light-strand promoter. *Proceedings of the National Academy of Sciences of the United States of America*, *82*(2), 351–355. https://doi.org/10.1073/pnas.82.2.351

Chujo, T., Ohira, T., Sakaguchi, Y., Goshima, N., Nomura, N., Nagao, A., & Suzuki, T. (2012). LRPPRC/SLIRP suppresses PNPase-mediated mRNA decay and promotes polyadenylation in human mitochondria. *Nucleic Acids Research*, *40*(16), 8033–8047. https://doi.org/10.1093/nar/gks506

Clayton, D. A. (1991). Replication and Transcription of Vertebrate Mitochondrial DNA. *Annual Review of Cell Biology*, *7*(1), 453–478. https://doi.org/10.1146/annurev.cb.07.110191.002321

D'Souza, A. R., & Minczuk, M. (2018, July 20). Mitochondrial transcription and translation: Overview. *Essays in Biochemistry*, Vol. 62, pp. 309–320. https://doi.org/10.1042/EBC20170102

Delettre, C., Lenaers, G., Griffoin, J. M., Gigarel, N., Lorenzo, C., Belenguer, P., … Hamel, C. P. (2000). Nuclear gene OPA1, encoding a mitochondrial dynamin-related protein, is mutated in dominant optic atrophy. *Nature Genetics*, *26*(2), 207–210. https://doi.org/10.1038/79936

Devall, M., Smith, R. G., Jeffries, A., Hannon, E., Davies, M. N., Schalkwyk, L., … Lunnon, K. (2017). Regional differences in mitochondrial DNA methylation in human post-mortem

brain tissue. *Clinical Epigenetics*, *9*(1). https://doi.org/10.1186/s13148-017-0337-3

Di Francesco, A., Arosio, B., Falconi, A., Micioni Di Bonaventura, M. V., Karimi, M., Mari, D., … D'Addario, C. (2015). Global changes in DNA methylation in Alzheimer's disease peripheral blood mononuclear cells. *Brain, Behavior, and Immunity*, *45*, 139–144. https://doi.org/10.1016/j.bbi.2014.11.002

Doda, J. N., Wright, C. T., & Clayton, D. A. (1981). Elongation of displacement-loop strands in human and mouse mitochondrial DNA is arrested near specific template sequences. *Proceedings of the National Academy of Sciences of the United States of America*, *78*(10 I), 6116–6120. https://doi.org/10.1073/pnas.78.10.6116

Dzitoyeva, S., Chen, H., & Manev, H. (2012). Effect of aging on 5-hydroxymethylcytosine in brain mitochondria. *Neurobiology of Aging*, *33*(12), 2881–2891. https://doi.org/10.1016/j.neurobiolaging.2012.02.006

Falkenberg, M. (2018, July 20). Mitochondrial DNA replication in mammalian cells: Overview of the pathway. *Essays in Biochemistry*, Vol. 62, pp. 287–296. https://doi.org/10.1042/EBC20170100

Farge, G., Mehmedovic, M., Baclayon, M., vandenWildenberg, S. M. J. L., Roos, W. H., Gustafsson, C. M., … Falkenberg, M. (2014). In Vitro-reconstituted nucleoids can block mitochondrial DNA replication and transcription. *Cell Reports*, *8*(1), 66–74. https://doi.org/10.1016/j.celrep.2014.05.046

Fernandez-Silva, P., Martinez-Azorin, F., Micol, V., & Attardi, G. (1997). The human mitochondrial transcription termination factor (mTERF) is a multizipper protein but binds to DNA as a monomer, with evidence pointing to intramolecular leucine zipper interactions. *EMBO Journal*, *16*(5), 1066–1079. https://doi.org/10.1093/emboj/16.5.1066

Frommer, M., McDonald, L. E., Millar, D. S., Collis, C. M., Watt, F., Grigg, G. W., … Paul, C. L. (1992). A genomic sequencing protocol that yields a positive display of 5-methylcytosine residues in individual DNA strands. *Proceedings of the National Academy of Sciences of the United States of America*, *89*(5), 1827–1831. https://doi.org/10.1073/pnas.89.5.1827

Fusté, J. M., Wanrooij, S., Jemt, E., Granycome, C. E., Cluett, T. J., Shi, Y., … Falkenberg, M. (2010). Mitochondrial RNA Polymerase Is Needed for Activation of the Origin of Light-Strand DNA Replication. *Molecular Cell*, *37*(1), 67–78. https://doi.org/10.1016/j.molcel.2009.12.021

Gaur, R., Grasso, D., Datta, P. P., Krishna, P. D. V., Das, G., Spencer, A., … Varshney, U. (2008). A Single Mammalian Mitochondrial Translation Initiation Factor Functionally Replaces Two Bacterial Factors. *Molecular Cell*, *29*(2), 180–190. https://doi.org/10.1016/j.molcel.2007.11.021

Giles, R. E., Blanc, H., Cann, H. M., & Wallace aD., C. (1980). Maternal inheritance of human mitochondrial DNA. *Proceedings of the National Academy of Sciences of the United States of America*, *77*(11 I), 6715–6719. https://doi.org/10.1073/pnas.77.11.6715

Gustafsson, C. M., Falkenberg, M., & Larsson, N.-G. (2016). Maintenance and Expression of Mammalian Mitochondrial DNA. *Annual Review of Biochemistry*, *85*(1), 133–160. https://doi.org/10.1146/annurev-biochem-060815-014402

Hällberg, B. M., & Larsson, N. G. (2014, August 5). Making proteins in the powerhouse. *Cell Metabolism*, Vol. 20, pp. 226–240. https://doi.org/10.1016/j.cmet.2014.07.001

Hammarsund, M., Wilson, W., Corcoran, M., Merup, M., Einhorn, S., Grandér, D., & Sangfelt, O. (2001). Identification and characterization of two novel human mitochondrial elongation

factor genes, hEFG2 and hEFG1, phylogenetically conserved through evolution. *Human Genetics*, *109*(5), 542–550. https://doi.org/10.1007/s00439-001-0610-5

Haque, M. E., & Spremulli, L. L. (2008). Roles of the N- and C-Terminal Domains of Mammalian Mitochondrial Initiation Factor 3 in Protein Biosynthesis. *Journal of Molecular Biology*, *384*(4), 929–940. https://doi.org/10.1016/j.jmb.2008.09.077

Hayashi, J. I., Ohta, S., Kikuchi, A., Takemitsu, M., Goto, Y. I., & Nonaka, I. (1991). Introduction of disease-related mitochondrial DNA deletions into HeLa cells lacking mitochondrial DNA results in mitochondrial dysfunction. *Proceedings of the National Academy of Sciences of the United States of America*, *88*(23), 10614–10618. https://doi.org/10.1073/pnas.88.23.10614

Hillen, H. S., Parshin, A. V., Agaronyan, K., Morozov, Y. I., Graber, J. J., Chernev, A., … Temiakov, D. (2017). Mechanism of Transcription Anti-termination in Human Mitochondria. *Cell*, *171*(5), 1082-1093.e13. https://doi.org/10.1016/j.cell.2017.09.035

Hohos, N. M., Lee, K., Ji, L., Yu, M., Kandasamy, M. M., Phillips, B. G., … Meagher, R. B. (2016). DNA cytosine hydroxymethylation levels are distinct among non-overlapping classes of peripheral blood leukocytes. *Journal of Immunological Methods*, *436*, 1–15. https://doi.org/10.1016/j.jim.2016.05.003

Hong, E. E., Okitsu, C. Y., Smith, A. D., & Hsieh, C.-L. (2013). Regionally Specific and Genome-Wide Analyses Conclusively Demonstrate the Absence of CpG Methylation in Human Mitochondrial DNA. *Molecular and Cellular Biology*, *33*(14), 2683–2690. https://doi.org/10.1128/mcb.00220-13

Jacobson, J., & Duchen, M. R. (2004, January). Interplay between mitochondria and cellular calcium signalling. *Molecular and Cellular Biochemistry*, Vol. 256–257, pp. 209–218.

https://doi.org/10.1023/b:mcbi.0000009869.29827.df

James, P., Sajjadi, S., Tomar, A. S., Saffari, A., Fall, C. H. D., Prentice, A. M., … Chandak, G. R. (2018). Candidate genes linking maternal nutrient exposure to offspring health via DNA methylation: A review of existing evidence in humans with specific focus on one-carbon metabolism. *International Journal of Epidemiology*, *47*(6), 1910–1937. https://doi.org/10.1093/ije/dyy153

Janssen, B. G., Byun, H. M., Cox, B., Gyselaers, W., Izzi, B., Baccarelli, A. A., & Nawrot, T. S. (2014). Variation of DNA methylation in candidate age-related targets on the mitochondrial-telomere axis in cord blood and placenta. *Placenta*, *35*(9), 665–672. https://doi.org/10.1016/j.placenta.2014.06.371

Janssen, Bram G., Byun, H. M., Gyselaers, W., Lefebvre, W., Baccarelli, A. A., & Nawrot, T. S. (2015). Placental mitochondrial methylation and exposure to airborne particulate matter in the early life environment: An ENVIRONAGE birth cohort study. *Epigenetics*, *10*(6), 536–544. https://doi.org/10.1080/15592294.2015.1048412

Javierre, B. M., Fernandez, A. F., Richter, J., Al-Shahrour, F., Ignacio Martin-Subero, J., Rodriguez-Ubreva, J., … Ballestar, E. (2010). Changes in the pattern of DNA methylation associate with twin discordance in systemic lupus erythematosus. *Genome Research*, *20*(2), 170–179. https://doi.org/10.1101/gr.100289.109

Jemt, E., Persson, Ö., Shi, Y., Mehmedovic, M., Uhler, J. P., López, M. D., … Falkenberg, M. (2015). Regulation of DNA replication at the end of the mitochondrial D-loop involves the helicase TWINKLE and a conserved sequence element. *Nucleic Acids Research*, *43*(19), 9262–9275. https://doi.org/10.1093/nar/gkv804

Jia, Y., Song, H., Gao, G., Cai, D., Yang, X., & Zhao, R. (2015). Maternal Betaine

Supplementation during Gestation Enhances Expression of mtDNA-Encoded Genes through D-Loop DNA Hypomethylation in the Skeletal Muscle of Newborn Piglets. *Journal of Agricultural and Food Chemistry*, *63*(46), 10152–10160. https://doi.org/10.1021/acs.jafc.5b04418

Jourdain, A. A., Koppen, M., Rodley, C. D., Maundrell, K., Gueguen, N., Reynier, P., … Martinou, J. C. (2015). A Mitochondria-Specific Isoform of FASTK Is Present In Mitochondrial RNA Granules and Regulates Gene Expression and Function. *Cell Reports*, *10*(7), 1110–1121. https://doi.org/10.1016/j.celrep.2015.01.063

Karbowski, M., Arnoult, D., Chen, H., Chan, D. C., Smith, C. L., & Youle, R. J. (2004). Quantitation of mitochondrial dynamics by photolabeling of individual organelles shows that mitochondrial fusion is blocked during the Bax activation phase of apoptosis. *Journal of Cell Biology*, *164*(4), 493–499. https://doi.org/10.1083/jcb.200309082

Kaufman, B. A., Durisic, N., Mativetsky, J. M., Costantino, S., Hancock, M. A., Grutter, P., & Shoubridge, E. A. (2007). The mitochondrial transcription factor TFAM coordinates the assembly of multiple DNA molecules into nucleoid-like structures. *Molecular Biology of the Cell*, *18*(9), 3225–3236. https://doi.org/10.1091/mbc.e07-05-0404

Kelly, R. D. W., Mahmud, A., McKenzie, M., Trounce, I. A., & St John, J. C. (2012). Mitochondrial DNA copy number is regulated in a tissue specific manner by DNA methylation of the nuclear-encoded DNA polymerase gamma A. *Nucleic Acids Research*, *40*(20), 10124–10138. https://doi.org/10.1093/nar/gks770

Koh, C. W. Q., Goh, Y. T., Toh, J. D. W., Neo, S. P., Ng, S. B., Gunaratne, J., … Goh, W. S. S. (2018). Single-nucleotide-resolution sequencing of human N 6 -methyldeoxyadenosine reveals strand-asymmetric clusters associated with SSBP1 on the mitochondrial genome.

Nucleic Acids Research, *46*(22), 11659–11670. https://doi.org/10.1093/nar/gky1104

Kukat, C., Davies, K. M., Wurm, C. A., Spåhr, H., Bonekamp, N. A., Kühl, I., … Larsson, N. G. (2015). Cross-strand binding of TFAM to a single mtDNA molecule forms the mitochondrial nucleoid. *Proceedings of the National Academy of Sciences of the United States of America*, *112*(36), 11288–11293. https://doi.org/10.1073/pnas.1512131112

Kukat, C., Wurm, C. A., Spåhr, H., Falkenberg, M., Larsson, N. G., & Jakobs, S. (2011). Super-resolution microscopy reveals that mammalian mitochondrial nucleoids have a uniform size and frequently contain a single copy of mtDNA. *Proceedings of the National Academy of Sciences of the United States of America*, *108*(33), 13534–13539. https://doi.org/10.1073/pnas.1109263108

Lakshmipathy, U., & Campbell, C. (1999). The Human DNA Ligase III Gene Encodes Nuclear and Mitochondrial Proteins. *Molecular and Cellular Biology*, *19*(5), 3869–3876. https://doi.org/10.1128/mcb.19.5.3869

Lee, S. R., & Han, J. (2017). Mitochondrial Nucleoid: Shield and Switch of the Mitochondrial Genome. *Oxidative Medicine and Cellular Longevity*, Vol. 2017. https://doi.org/10.1155/2017/8060949

Li, B., Kaushik, S., Kalinowski, P., Kim, B. R., Gershome, C., Ching, J., & Poburko, D. (2018). Droplet digital PCR shows the D-Loop to be an error prone locus for mitochondrial DNA copy number determination. *Scientific Reports*, *8*(1), 1–13. https://doi.org/10.1038/s41598-018-29621-1

Li, P., Nijhawan, D., Budihardjo, I., Srinivasula, S. M., Ahmad, M., Alnemri, E. S., & Wang, X. (1997). Cytochrome c and dATP-dependent formation of Apaf-1/caspase-9 complex initiates an apoptotic protease cascade. *Cell*, *91*(4), 479–489. https://doi.org/10.1016/S0092-

8674(00)80434-1

Liao, K., Yan, J., Mai, K., & Ai, Q. (2016). Dietary lipid concentration affects liver mitochondrial DNA copy number, gene expression and DNA methylation in large yellow croaker (Larimichthys crocea). *Comparative Biochemistry and Physiology Part B: Biochemistry and Molecular Biology*, *193*, 25–32. https://doi.org/10.1016/j.cbpb.2015.11.012

Lightowlers, R. N., Chinnery, P. F., Turnbull, D. M., Howell, N., & Turnbuu, D. M. (1997). Mammalian mitochondrial genetics: Heredity, heteroplasmy and disease. *Trends in Genetics*, Vol. 13, pp. 450–455. https://doi.org/10.1016/S0168-9525(97)01266-3

Linqing, Y., Bo, X., Xueqin, Y., Hong, D., Desheng, W., Huimin, Z., … Zhixiong, Z. (2016). Mitochondrial DNA hypomethylation in chrome plating workers. *Toxicology Letters*, *243*, 1–6. https://doi.org/10.1016/j.toxlet.2015.11.031

Liu, B., Du, Q., Chen, L., Fu, G., Li, S., Fu, L., … Bin, C. (2016). CpG methylation patterns of human mitochondrial DNA. *Scientific Reports*. https://doi.org/10.1038/srep23421

Lyko, F. (2018, February 1). The DNA methyltransferase family: A versatile toolkit for epigenetic regulation. *Nature Reviews Genetics*, Vol. 19, pp. 81–92. https://doi.org/10.1038/nrg.2017.80

Martin, W. F., Garg, S., & Zimorski, V. (2015, September 26). Endosymbiotic theories for eukaryote origin. *Philosophical Transactions of the Royal Society B: Biological Sciences*, Vol. 370. https://doi.org/10.1098/rstb.2014.0330

Maude, H., Davidson, M., Charitakis, N., Diaz, L., Bowers, W. H. T., Gradovich, E., … Huntley, D. (2019). NUMT confounding biases mitochondrial heteroplasmy calls in favor of the reference allele. *Frontiers in Cell and Developmental Biology*, *7*(SEP).

https://doi.org/10.3389/fcell.2019.00201

Mechta, M., Ingerslev, L. R., Fabre, O., Picard, M., & Barrès, R. (2017). Evidence suggesting absence of mitochondrial DNA methylation. *Frontiers in Genetics*, *8*(NOV). https://doi.org/10.3389/fgene.2017.00166

Miralles Fusté, J., Shi, Y., Wanrooij, S., Zhu, X., Jemt, E., Persson, Ö., … Falkenberg, M. (2014). In Vivo Occupancy of Mitochondrial Single-Stranded DNA Binding Protein Supports the Strand Displacement Mode of DNA Replication. *PLoS Genetics*, *10*(12), e1004832. https://doi.org/10.1371/journal.pgen.1004832

Mishra, M., & Kowluru, R. A. (2015). Epigenetic modification of mitochondrial DNA in the development of diabetic retinopathy. *Investigative Ophthalmology and Visual Science*, *56*(9), 5133–5142. https://doi.org/10.1167/iovs.15-16937

Mohn, F., Weber, M., Schübeler, D., & Roloff, T. C. (2009). Methylated DNA immunoprecipitation (MeDIP). *Methods in Molecular Biology (Clifton, N.J.)*, *507*, 55–64. https://doi.org/10.1007/978-1-59745-522-0_5

Montoya, J., Christianson, T., Levens, D., Rabinowitz, M., & Attardi, G. (1982). Identification of initiation sites for heavy-strand and light-strand transcription in human mitochondrial DNA. *Proceedings of the National Academy of Sciences of the United States of America*, *79*(23 I), 7195–7199. https://doi.org/10.1073/pnas.79.23.7195

Nass, M. M. K. (1973). Differential methylation of mitochondrial and nuclear DNA in cultured mouse, hamster and virus-transformed hamster cells In vivo and in vitro methylation. *Journal of Molecular Biology*, *80*(1), 155–175. https://doi.org/10.1016/0022-2836(73)90239-8

Ngo, H. B., Kaiser, J. T., & Chan, D. C. (2011). The mitochondrial transcription and packaging

factor Tfam imposes a U-turn on mitochondrial DNA. *Nature Structural and Molecular Biology*, *18*(11), 1290–1296. https://doi.org/10.1038/nsmb.2159

Nicholls, T. J., & Minczuk, M. (2014). In D-loop: 40 years of mitochondrial 7S DNA. *Experimental Gerontology*, *56*, 175–181. https://doi.org/10.1016/j.exger.2014.03.027

Ojala, D., Montoya, J., & Attardi, G. (1981). TRNA punctuation model of RNA processing in human mitochondria. *Nature*, *290*(5806), 470–474. https://doi.org/10.1038/290470a0

Owa, C., Poulin, M., Yan, L., & Shioda, T. (2018). Technical adequacy of bisulfite sequencing and pyrosequencing for detection of mitochondrial DNA methylation: Sources and avoidance of false-positive detection. *PLoS ONE*, *13*(2). https://doi.org/10.1371/journal.pone.0192722

Patil, V., Cuenin, C., Chung, F., Aguilera, J. R. R., Fernandez-Jimenez, N., Romero-Garmendia, I., … Herceg, Z. (2019). Human mitochondrial DNA is extensively methylated in a non-CpG context. *Nucleic Acids Research*, *47*(19), 10072–10085. https://doi.org/10.1093/nar/gkz762

Pirola, C. J., Fernández Gianotti, T., Burgueño, A. L., Rey-Funes, M., Loidl, C. F., Mallardi, P., … Sookoian, S. (2013). Epigenetic modification of liver mitochondrial DNA is associated with histological severity of nonalcoholic fatty liver disease. *Gut*, *62*(9), 1356–1363. https://doi.org/10.1136/gutjnl-2012-302962

Pollack, Y., Kasir, J., Shemer, R., Metzger, S., & Szyf, M. (1984). Methylation pattern of mouse mitochondrial DNA. *Nucleic Acids Research*, *12*(12), 4811–4824. https://doi.org/10.1093/nar/12.12.4811

Prachař, J. (2016). Ultrastructure of mitochondrial nucleoid and its surroundings. *General Physiology and Biophysics*, *35*(03), 273–286. https://doi.org/10.4149/gpb_2016008

Rappaport, L., Oliviero, P., & Samuel, J. L. (1998). Cytoskeleton and mitochondrial morphology and function. *Molecular and Cellular Biochemistry,* Vol. 184, pp. 101–105. https://doi.org/10.1007/978-1-4615-5653-4_8

Robin, E. D., & Wong, R. (1988). Mitochondrial DNA molecules and virtual number of mitochondria per cell in mammalian cells. *Journal of Cellular Physiology*, *136*(3), 507–513. https://doi.org/10.1002/jcp.1041360316

Rorbach, J., Richter, R., Wessels, H. J., Wydro, M., Pekalski, M., Farhoud, M., … Chrzanowska-Lightowlers, Z. M. A. (2008). The human mitochondrial ribosome recycling factor is essential for cell viability. *Nucleic Acids Research*, *36*(18), 5787–5799. https://doi.org/10.1093/nar/gkn576

Ruzzenente, B., Metodiev, M. D., Wredenberg, A., Bratic, A., Park, C. B., Cámara, Y., … Larsson, N. G. (2012). LRPPRC is necessary for polyadenylation and coordination of translation of mitochondrial mRNAs. *EMBO Journal*, *31*(2), 443–456. https://doi.org/10.1038/emboj.2011.392

Santel, A., & Fuller, M. T. (2001). Control of mitochondrial morphology by a human mitofusin. *Journal of Cell Science*, *114*(5), 867–874.

Sanyal, T., Bhattacharjee, P., Bhattacharjee, S., & Bhattacharjee, P. (2018). Hypomethylation of mitochondrial D-loop and ND6 with increased mitochondrial DNA copy number in the arsenic-exposed population. *Toxicology*, *408*, 54–61. https://doi.org/10.1016/j.tox.2018.06.012

Serre, D., Lee, B. H., & Ting, A. H. (2010). MBD-isolated Genome Sequencing provides a high-throughput and comprehensive survey of DNA methylation in the human genome. *Nucleic Acids Research*, *38*(2), 391–399. https://doi.org/10.1093/nar/gkp992

Shmookler Reis, R. J., & Goldstein, S. (1983). Mitochondrial DNA in mortal and immortal human cells. Genome number, integrity, and methylation. *Journal of Biological Chemistry*, *258*(15), 9078–9085.

Shock, L. S., Thakkar, P. V., Peterson, E. J., Moran, R. G., & Taylor, S. M. (2011). DNA methyltransferase 1, cytosine methylation, and cytosine hydroxymethylation in mammalian mitochondria. *Proceedings of the National Academy of Sciences*. https://doi.org/10.1073/pnas.1012311108

Silva, M. F. B., Aires, C. C. P., Luis, P. B. M., Ruiter, J. P. N., IJlst, L., Duran, M., … Tavares de Almeida, I. (2008). Valproic acid metabolism and its effects on mitochondrial fatty acid oxidation: A review. *Journal of Inherited Metabolic Disease*, *31*(2), 205–216. https://doi.org/10.1007/s10545-008-0841-x

Smiraglia, D. J., Kulawiec, M., Bistulfi, G. L., Gupta, S. G., & Singh, K. K. (2008). A novel role for mitochondria in regulating epigenetic modification in the nucleus. *Cancer Biology and Therapy*, *7*(8), 1182–1190. https://doi.org/10.4161/cbt.7.8.6215

Soleimanpour-Lichaei, H. R., Kühl, I., Gaisne, M., Passos, J. F., Wydro, M., Rorbach, J., … Chrzanowska-Lightowlers, Z. (2007). mtRF1a Is a Human Mitochondrial Translation Release Factor Decoding the Major Termination Codons UAA and UAG. *Molecular Cell*, *27*(5), 745–757. https://doi.org/10.1016/j.molcel.2007.06.031

Spencer, A. C., & Spremulli, L. L. (2004). Interaction of mitochondrial initiation factor 2 with mitochondrial fMet-tRNA. *Nucleic Acids Research*, *32*(18), 5464–5470. https://doi.org/10.1093/nar/gkh886

Sterky, F. H., Ruzzenente, B., Gustafsson, C. M., Samuelsson, T., & Larsson, N.-G. (2010). LRPPRC is a mitochondrial matrix protein that is conserved in metazoans. *Biochemical and*

Biophysical Research Communications, *398*(4), 759–764. https://doi.org/10.1016/j.bbrc.2010.07.019

Terry, M. B., Delgado-Cruzata, L., Vin-Raviv, N., Wu, H. C., & Santella, R. M. (2011). DNA methylation in white blood cells. *Epigenetics*, *6*(7), 828–837. https://doi.org/10.4161/epi.6.7.16500

Tomecki, R. (2004). Identification of a novel human nuclear-encoded mitochondrial poly(A) polymerase. *Nucleic Acids Research*, *32*(20), 6001–6014. https://doi.org/10.1093/nar/gkh923

Unnikrishnan, A., Freeman, W. M., Jackson, J., Wren, J. D., Porter, H., & Richardson, A. (2019, March 1). The role of DNA methylation in epigenetics of aging. *Pharmacology and Therapeutics*, Vol. 195, pp. 172–185. https://doi.org/10.1016/j.pharmthera.2018.11.001

Van Der Wijst, M. G. P., Van Tilburg, A. Y., Ruiters, M. H. J., & Rots, M. G. (2017). Experimental mitochondria-targeted DNA methylation identifies GpC methylation, not CpG methylation, as potential regulator of mitochondrial gene expression. *Scientific Reports*, *7*(1). https://doi.org/10.1038/s41598-017-00263-z

Wakae, K., Nishiyama, T., Kondo, S., Izuka, T., Que, L., Chen, C., … Muramatsu, M. (2018). Keratinocyte differentiation induces APOBEC3A, 3B, and mitochondrial DNA hypermutation. *Scientific Reports*, *8*(1). https://doi.org/10.1038/s41598-018-27930-z

Wallace, D. C., Fan, W., & Procaccio, V. (2010). Mitochondrial Energetics and Therapeutics. *Annual Review of Pathology: Mechanisms of Disease*, *5*(1), 297–348. https://doi.org/10.1146/annurev.pathol.4.110807.092314

Williams, R. S. (1986). Mitochondrial gene expression in mammalian striated muscle. Evidence that variation in gene dosage is the major regulatory event. *Journal of Biological Chemistry*,

261(26), 12390–12394. Retrieved from http://www.jbc.org/content/261/26/12390.short

Woischnik, M., & Moraes, C. T. (2002). Pattern of Organization of Human Mitochondrial Pseudogenes in the Nuclear Genome. *Genome Research*, *12*(6), 885–893. https://doi.org/10.1101/gr.227202

Wolters, J. E. J., Van Breda, S. G. J., Caiment, F., Claessen, S. M., De Kok, T. M. C. M., & Kleinjans, J. C. S. (2017). Nuclear and Mitochondrial DNA Methylation Patterns Induced by Valproic Acid in Human Hepatocytes. *Chemical Research in Toxicology*, *30*(10), 1847–1854. https://doi.org/10.1021/acs.chemrestox.7b00171

Wong, M., Gertz, B., Chestnut, B. A., & Martin, L. J. (2013). Mitochondrial DNMT3A and DNA methylation in skeletal muscle and CNS of transgenic mouse models of ALS. *Frontiers in Cellular Neuroscience*, *7*(DEC). https://doi.org/10.3389/fncel.2013.00279

Wu, H. C., Delgado-Cruzata, L., Flom, J. D., Kappil, M., Ferris, J. S., Liao, Y., … Terry, M. B. (2011). Global methylation profles in DNA from different blood cell types. *Epigenetics*, *6*(1), 76–85. https://doi.org/10.4161/epi.6.1.13391

Wu, X., & Zhang, Y. (2017, September 1). TET-mediated active DNA demethylation: Mechanism, function and beyond. *Nature Reviews Genetics*, Vol. 18, pp. 517–534. https://doi.org/10.1038/nrg.2017.33

Xiao, C. Le, Zhu, S., He, M., Chen, D., Zhang, Q., Chen, Y., … Yan, G. R. (2018). N 6 - Methyladenine DNA Modification in the Human Genome. *Molecular Cell*, *71*(2), 306-318.e7. https://doi.org/10.1016/j.molcel.2018.06.015

Xuan, H. P., Farge, G., Shi, Y., Gaspari, M., Gustafsson, C. M., & Falkenberg, M. (2006). Conserved sequence box II directs transcription termination and primer formation in mitochondria. *Journal of Biological Chemistry*, *281*(34), 24647–24652.

https://doi.org/10.1074/jbc.M602429200

Yakubovskaya, E., Guja, K. E., Eng, E. T., Choi, W. S., Mejia, E., Beglov, D., … Garcia-Diaz, M. (2014). Organization of the human mitochondrial transcription initiation complex. *Nucleic Acids Research*, *42*(6), 4100–4112. https://doi.org/10.1093/nar/gkt1360

Yoon, Y., Krueger, E. W., Oswald, B. J., & McNiven, M. A. (2003). The Mitochondrial Protein hFis1 Regulates Mitochondrial Fission in Mammalian Cells through an Interaction with the Dynamin-Like Protein DLP1. *Molecular and Cellular Biology*, *23*(15), 5409–5420. https://doi.org/10.1128/mcb.23.15.5409-5420.2003

Yu, M., Hon, G. C., Szulwach, K. E., Song, C. X., Zhang, L., Kim, A., … He, C. (2012). Base-resolution analysis of 5-hydroxymethylcytosine in the mammalian genome. *Cell*, *149*(6), 1368–1380. https://doi.org/10.1016/j.cell.2012.04.027

Züchner, S., Mersiyanova, I. V., Muglia, M., Bissar-Tadmouri, N., Rochelle, J., Dadali, E. L., … Vance, J. M. (2004). Mutations in the mitochondrial GTPase mitofusin 2 cause Charcot-Marie-Tooth neuropathy type 2A. *Nature Genetics*, *36*(5), 449–451. https://doi.org/10.1038/ng1341

APPENDICES

APPENDIX A: Research Ethics Board Certificate of Approval

P126-770 Bannatyne Avenue
Winnipeg, Manitoba
Canada, R3E 0W3
Telephone : 204-789-3255
Fax: 204-789-3414

UNIVERSITY OF MANITOBA | Research Ethics - Bannatyne
Office of the Vice-President (Research and International)

HEALTH RESEARCH ETHICS BOARD (HREB)
CERTIFICATE OF FINAL APPROVAL FOR NEW STUDIES
Full Board Review

PRINCIPAL INVESTIGATOR:	INSTITUTION/DEPARTMENT:	ETHICS #:
Dr. James Davie	U of M, CHRIM and BMG/Medicine	HS20757 (H2017:150)
HREB MEETING DATE:	**APPROVAL DATE:**	**EXPIRY DATE:**
April 24, 2017	May 23, 2017	**April 24, 2018**
STUDENT PRINCIPAL INVESTIGATOR SUPERVISOR (If applicable):		

PROTOCOL NUMBER:	PROJECT OR PROTOCOL TITLE:
NA	DNA Methylation Marks in Nuclear and Mitochondrial DNA
SPONSORING AGENCIES AND/OR COORDINATING GROUPS:	
Children's Hospital Research Institute of Manitoba (CHRIM)	

Submission Date(s) of Investigator Documents:	REB Receipt Date(s) of Documents:
March 30 and May 9, 2017	April 3 and May 10, 2017

THE FOLLOWING ARE APPROVED FOR USE:

Document Name	Version(if applicable)	Date
Protocol:		
Protocol		May 9, 2017
Clarification Letter dated May 9, 2017		
REB Submission Form signed May 10, 2017		
Consent and Assent Form(s):		
Research Participant Information and Consent Form		09/05/2017
Other:		

CERTIFICATION
The University of Manitoba (UM) Health Research Board (HREB) has reviewed the research study/project named on this ***Certificate of Final Approval*** at the ***full board meeting*** date noted above and was found to be acceptable on ethical grounds for research involving human participants. The study/project and documents listed above was granted final approval by the Chair or Acting Chair, UM HREB.

HREB ATTESTATION
The University of Manitoba (UM) Health Research Board (HREB) is organized and operates according to Health Canada/ICH Good Clinical Practices, Tri-Council Policy Statement 2, and the applicable laws and regulations of Manitoba. In respect to clinical trials, the HREB complies with the membership requirements for Research Ethics Boards defined in Division 5 of the Food and Drug Regulations of Canada and carries out its functions in a manner consistent with Good Clinical Practices.

QUALITY ASSURANCE
The University of Manitoba Research Quality Management Office may request to review research documentation from this research study/project to demonstrate compliance with this approved protocol and the University of Manitoba Policy on the Ethics of Research Involving Humans.

CONDITIONS OF APPROVAL:
1. The study is acceptable on scientific and ethical grounds for the ethics of human use only. ***For logistics of performing the study, approval must be sought from the relevant institution(s).***
2. This research study/project is to be conducted by the local principal investigator listed on this certificate of approval.
3. The principal investigator has the responsibility for any other administrative or regulatory approvals that may pertain to the research study/project, and for ensuring that the authorized research is carried out according to governing law.
4. **This approval is valid until the expiry date noted on this certificate of approval. A Bannatyne Campus Annual Study Status Report** must be submitted to the REB within 15-30 days of this expiry date.
5. Any changes of the protocol (including recruitment procedures, etc.), informed consent form(s) or documents must be reported to the HREB for consideration in advance of implementation of such changes on the **Bannatyne Campus Research Amendment Form.**
6. Adverse events and unanticipated problems must be reported to the REB as per Bannatyne Campus Research Boards Standard Operating procedures.
7. The UM HREB must be notified regarding discontinuation or study/project closure on the **Bannatyne Campus Final Study Status Report**.

[redacted]
Chair, Health Research Ethics Board
Bannatyne Campus

Please quote the above Human Ethics Number on all correspondence.
Inquiries should be directed to the REB Secretary **Telephone:** (204) 789-3255/ **Fax:** (204) 789-3414

APPENDIX B: Consent Form

Manitoba Institute of Child Health
513-715 McDermot Avenue, Winnipeg, MB R3E 3P4
(204) 789-3447 / Fax (204) 789-3915

RESEARCH PARTICIPANT INFORMATION AND CONSENT FORM

Title of Study: DNA Methylation Marks in Nuclear and Mitochondrial DNA.

Principal Investigator:
Dr. James Davie, Department of Biochemistry and Medical Genetics, University of Manitoba, 600A-715 McDermot Ave, R3E 3P4, Winnipeg, MB, phone: 204-975-7732.

Co-Investigators:
Dr. Vern Dolinsky, Department of Pharmacology and Therapeutics, University of Manitoba, 601 JBRC -715 McDermot Ave, R3E 3P4, Winnipeg, MB, phone: 204-789-3559.
Dr. Joe Gordon, Department of Human Anatomy and Cell Science, University of Manitoba, 561 JBRC-715 McDermot Ave, R3E 3P4, Winnipeg, MB, phone: 204-474-6668.
Dr. Brandy Wicklow, Department of Pediatric and Child Health, University of Manitoba, FE- 307 685 William Ave, R3E 0Z2, Winnipeg, MB, phone: 204-787-3011.

Sponsor: N/A

You are being asked to participate in a research study. Please take your time to review this consent form and discuss any questions you may have with the study staff. You may take your time to make your decision about participating in this study and you may discuss it with your friends, family or (if applicable) your doctor before you make your decision. This consent form may contain words that you do not understand. Please ask the study staff to explain any words or information that you do not clearly understand.

Purpose of Study

This research study is being conducted to test and determine which of the multitude of methods of measuring the nuclear and mitochondrial epigenetic marker 5-hydroxymethylcytosine (5-hmC) in peripheral blood mononuclear cells is more efficient, reliable and cost effective. It is well established that the methylation of cytosine (5-mC) on the DNA in the regulatory regions of genes has a negative effect on gene expression. Recently, studies have shown that another epigenetic mark, hydroxymethylation of cytosine (5-hmC), has a positive effect on gene expression and researchers are currently establishing it as a biomarker of disease. Additionally, studies have shown that mitochondrial DNA is modified by both methylation and hydroxymethylation and that although methylation of cytosine (5-mC) in mitochondrial DNA is conserved across tissue types, hydroxymethylation appears more dynamic and therefore may have some role in regulation of mitochondrial gene expression. Our objective is to see if the incorporation of 5-hmC in both nuclear and mitochondrial DNA to that of 5-mC would provide a better biomarker. In order to accomplish that goal, the best method of measuring 5-hmC must be determined.

A total of 12 healthy volunteer research participants will participate in this study.

Study Procedures

If you take part in this study, you will have the following procedures:
There will be one up to two blood draws on separate occasions. At each single draw, 5 ml (1 teaspoon) of venous blood sample will be collected in EDTA tubes at the Developmental Origins of Health and Disease (DOHaD) monthly meeting at CHRIM by a trained medical professional from the Clinical Research Unit. Some of the specimens can be stored for up to a year at -80 degree Celsius in 624 JBRC and only the principal investigator and study staff will be allowed to access the stored specimens. Peripheral blood mononuclear cells (PBMCs) will be isolated from the blood using two methods: one method uses fresh whole blood samples with controlled red blood cell lysis and the other uses frozen whole blood samples. The distribution and content of 5-hmC appears to be variable among the cell types in the PBMCs and it has been shown in a recent study that CD4+ helper T cells have the highest level of 5-hmC among other types of leukocytes whereas CD8+ cytotoxic T cells have low levels of 5-hmC but moderately high levels of 5-mC relative to other PBMCs. Therefore, our focus will initially be on the T cells (both CD4+ T helper cells and CD8+ T cytotoxic cells) for analyses of 5-hmC in nuclear and mitochondrial DNA and compare these results with unfractionated PBMCs. The magnetic beads with specific antibodies will be used to isolate the cells of interest (e.g. anti-CD8+ Dynabeads for CD8+ T cells). Following that, nuclear DNA, mitochondria and mitochondrial DNA will be isolated from T cells using the QIAGEN DNeasy Blood & Tissue Kit and the Abcam Mitochondrial DNA Isolation Kit, respectively.

There are multiple methods to isolate DNA regions with 5-hmC from isolated nuclear and mitochondrial DNA. Considering all the available methodologies, two methods will be initially applied and compared in terms of their efficiency and reliability in detecting 5-hmC regions using two kits from Active Motif: the Hydroxymethyl Collector Kit which has a range of detection between 1 µg and 10 µg of fragmented genomic DNA per capture reaction and the Hydroxymethylated DNA Immunoprecipitation (hMeDIP) Kit which includes a highly specific antibody for 5-hmC.

Participation in the study will be for one to two randomly separate days as it is limited to the donation of blood samples. You can stop participating at any time. However, if you decide to stop participating in the study, we encourage you to talk to the study staff first. There will not be any consequences of sudden withdrawal from the study.

No feedback will be provided as these samples will not be identified, just coded numerically, and therefore it will not be known whose data belongs to whom. The data will be stored on hard drives in the possession of the bioinformatician who does the analysis and as different bioinformatic tools become available, there may be further analysis done.

Risks and Discomforts

There may be temporary discomfort, a slight risk of infection, possible bruising, redness and swelling around the site of blood draw and you may feel lightheaded.

Benefits

There may not be direct benefit to you from participating in this study as the samples taken will be used only for research. We hope the information learned from this study will help determine which method for detecting 5-hmC is best to incorporate in another research project in the future.

Costs

All the procedures, which will be performed as part of this study, are provided at no cost to you.

Payment for Participation

You will receive no payment or reimbursement for any expenses related to taking part in this study.

Alternatives

The alternative to participation in our study is to not participate.

Confidentiality

No identifying information will be collected or used in this study. The specimens will bear only a randomly assigned study number; therefore, the study staff will not know whose sample belongs to whom. General information about what this research study finds may be published or presented in public forums; however, your name on this consent form will not be used or revealed.

Voluntary Participation/Withdrawal from the Study

Your decision to take part in this study is voluntary. You may refuse to participate, or you may withdraw from the study at any time. Your decision not to participate or to withdraw from the study will not affect your job standing or performance evaluation. If the study staff feel that it is in your best interest to withdraw you from the study, they will remove you without your consent.

Medical Care for Injury Related to the Study

In the case of injury or illness resulting from this study, necessary medical treatment will be available at no additional cost to you.

Questions

You are free to ask any questions that you may have about your participation and your rights as a research participant. If any questions come up during or after the study or if you have a research-related injury, contact the study coordinator: **Aleksandar Ilic** at **204-789-7733**.

For questions about your rights as a research participant, you may contact The University of

Manitoba, Bannatyne Campus Research Ethics Board Office at **204-789-3389**

Do not sign this consent form unless you have had a chance to ask questions and have received satisfactory answers to all of your questions.

Statement of Consent

I have read this consent form. I have had the opportunity to discuss this research study with Dr. James Davie and/or his study staff. I have had my questions answered by them in language I understand. The risks and benefits have been explained to me. I believe that I have not been unduly influenced by any study team member to participate in the research study by any statements or implied statements. Any relationship (such as employer, supervisor or family member) I may have with the study team has not affected my decision to participate. I understand that I will be given a copy of this consent form after signing it. I understand that my participation in this study is voluntary and that I may choose to withdraw at any time. I freely agree to participate in this research study.

By signing this consent form, I have not waived any of the legal rights that I have as a participant in a research study.

Participant signature: _____ **Date** _____
(day/month/year)

Participant printed name: _____

I, the undersigned, have fully explained the relevant details of this research study to the participant named above and believe that the participant has understood and has knowingly given their consent.

Printed Name: _____ **Date** _____
(day/month/year)

Signature: _____

Role in the study: _____

Relationship (if any) to study team members: _____